Deciphering the origin of dubiofossils from the Pennsylvanian of the Paraná Basin, Brazil

João Pedro Saldanha[1], Joice Cagliari[1], Rodrigo Scalise Horodyski[1], Lucas Del Mouro[2], Mírian Liza Alves Forancelli Pacheco[3]

5 [1]Programa de Pós-Graduação em Geologia, Universidade do Vale do Rio dos Sinos, São Leopoldo, RS, 93022-750, Brazil
[2]Instituto de Geociências, Universidade de São Paulo, São Paulo, SP, 05508-080, Brazil
[3]Departamento de Biologia, Universidade Federal de São Carlos - Campus Sorocaba, Sorocaba, SP, 18052-780, Brazil

Correspondence to: João Pedro Saldanha (saldanhajpedro@gmail.com)

Abstract. Minerals are the fundamental record of abiotic processes over time, while biominerals, are one of the most common
10 records of life due to their easy preservation and abundance. However, distinguishing between biominerals and abiotic minerals
is challenging because the record is defined by the superimposition and repetition of geologic processes and the interference
of ubiquitous and diverse life on Earth's surface and crust. Mineral dubiofossils, located on the threshold between abiotic and
biotic, can help resolve this issue. The aim of this contribution is to decipher the origin and history of branched mineralized
structures that were previously considered mineral dubiofossils. While this material has different forms and refers to biological
15 aspects, it is difficult to associate it with any known Fossil Group due to the overlapping geological processes that occur in the
Rio do Sul Formation (Pennsylvanian of the Paraná Basin), very close to the contact from a sill of the Serra Geral Group –
Lower Cretaceous with a proven thermal effect. The samples were described using a protocol that evaluated: 1) morphology,
texture, and structure; 2) relationship with the matrix; 3) composition and 4) context, assessing indigeneity and syngenicity,
and comparing them with abiotic and biotic products. Despite conducting an extensive comparison with abiotic minerals, as
20 well as controlled, induced, and influenced biominerals, no more probable hypothesis was found, excluding the possibility of
it being a controlled biomineral due to its patternless diversity of forms and the purely thermometamorphic origin due to the
branched elongated form. The occurrence of these structures suggests a complex history: a syndepositional or eodiagenetic
origin of some carbonate or sulfate (gypsum, ikaite, dolomite, calcite, siderite), which may be linked to the presence of
microbial mats, could have served as a template for mineralization and possibly mediated mineral growth. Mesodiagenesis
25 could have also modified the occurrence, but the main agent responsible for its formation was the Cretaceous intrusion, which
dissolved and replaced the initial mineral and precipitated calcite, resulting in the dubiofossil. Throughout these steps, physical-
chemical and biological reactions, aided by the intrinsic characteristics of the matrix, amount of organic matter, and distance
from contact with the intrusive body, may have increased the morphological complexity. This material illustrates how
dubiofossils can be the result of a complex history and overlapping geological processes. It also highlights the difficulty in
30 differentiating biominerals from abiotic minerals due to the scarcity of biogenicity arguments.

1 Introduction

Biogenicity refers to the signatures exclusively generated/transformed by past or present organisms. Comprising signs of morphology (structure, distribution, texture) and/or chemistry (composition and trace indicator) that diagnose life, these signatures can be created from the growth or decay of (once) living organisms and cannot be produced by purely abiotic

35   processes (Slater, 2009; McLoughlin, 2011). The issue lies in the ability to discriminate the origins of different components within complex mixtures, given the range of spatial scales, diversity of life forms, and succession of geologic processes (Schiffbauer et al., 2007; Botta et al., 2008; Neveu et al., 2018; Rouillard et al., 2021).

Ascertaining the biological origin and establishing solid evidence for biogenicity is preponderant (Neveu et al., 2018; Callefo et al., 2019a; Rouillard et al., 2021), especially to understand the biosphere-lithosphere interface (McMahon and Ivarsson,

40   2019). Life forms inhabit all environments on the planet's surface, including extreme environmental conditions (Fig. 1; Merino et al., 2019; McMahon and Ivarsson, 2019, and references therein). Thus, in addition to the traditional view that organisms are delimited and conditioned by environmental characteristics, the interference of life in natural processes and events have been increasingly proven (Knoll, 2013; Davies et al., 2020). Making it difficult to recognize large physical and chemical cycles on Earth that escape the biosphere activity (Gargaud et al., 2015) or even to measure the impact of the ubiquitous presence of

45   organisms on erosion, sedimentation, diagenesis, and mineralization (Fig. 1; Briggs, 2003; Dupraz et al., 2004; Gargaud et al., 2015; Knoll, 2013; Bower et al., 2015; Briggs and McMahon, 2016; McMahon and Ivarsson, 2019; Davies et al., 2020).
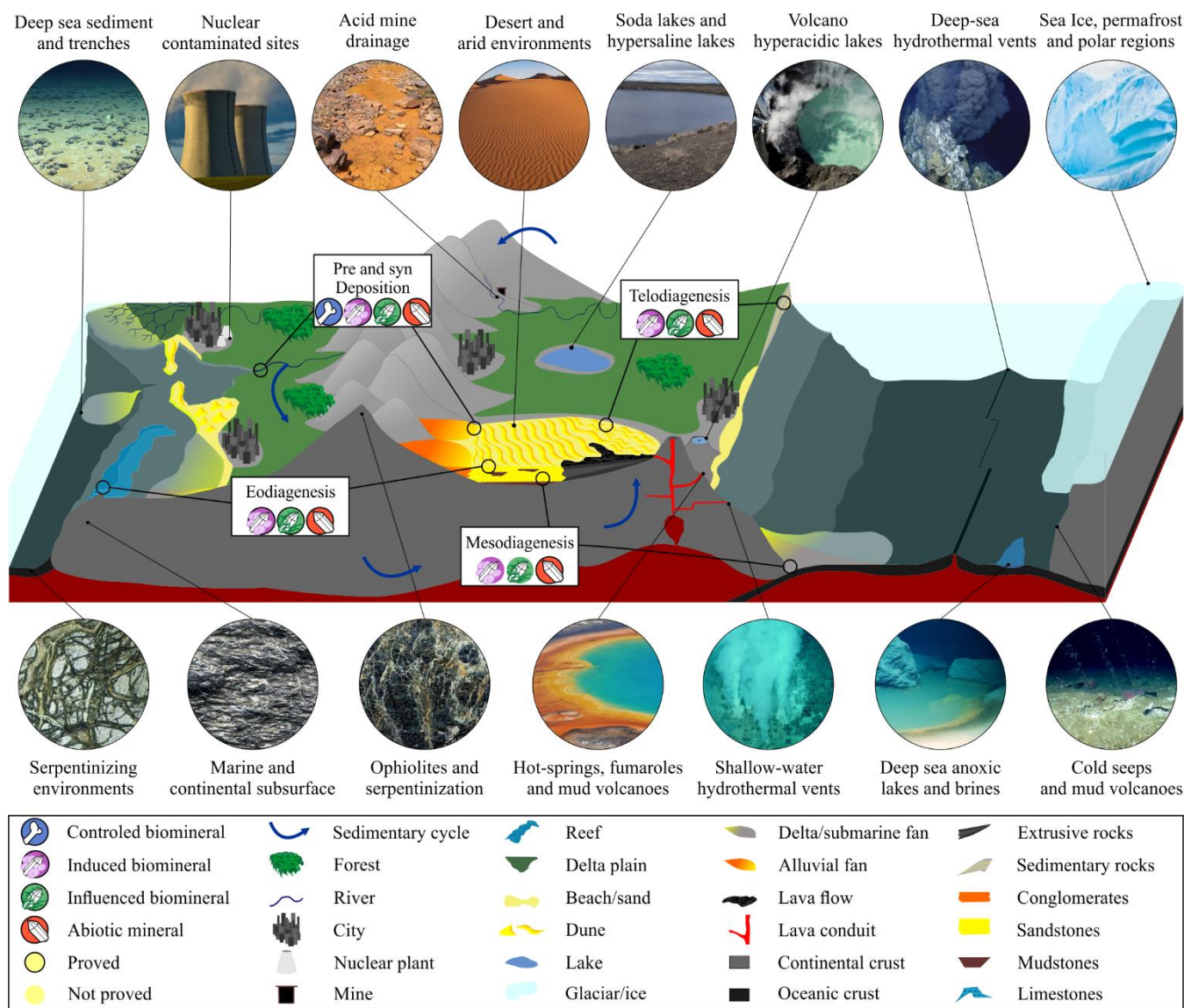
Figure 1: Representative cross-section of Earth's crust showing the diversity of inhabited extreme environments and the contribution of abiotic and biotic minerals in the sedimentary cycle. Induced/influenced biominerals may be present in the diagenesis cycle, including mesodiagenesis. Adapted from Dupraz et al. (2009), McMahon and Ivarsson (2019), and Merino et al. (2019).

50   These biological and geological processes are part of the natural cycles of the Earth system and therefore tend to repeat and

overlap on multiple scales (Zhang et al., 2017). A dynamic scenario of physical, chemical, and biological reactions occurs

throughout the Earth's crust and surface define the record (Milliken, 1978; Jacobson et al., 2000; Worden and Burley, 2009;

Zhang et al., 2017). Accordingly, a geological object whether abiotic or biotic must be understood as a result of its formation

and origin conditions added to all the subsequent processes involved that maintain, modify, or destroy it. Therefore, due to the
55   narrow threshold between biotic and abiotic environments, the superimposition of processes and continuous changes through
the geologic history, it is necessary to discriminate specific life signatures (Schiffbauer et al., 2007; Knoll, 2013; McLoughlin
and Grosch, 2015; Neveu et al., 2018; McMahon et al., 2021; Rouillard et al., 2021).

As they are on the threshold of knowledge between abiotic and biotic, dubiofossils, fossil-like structures formerly related to
life with an ambiguous origin (Hofmann, 1972), hold promising potential for enhancing biosignatures. Only when the
60   biological origin of a dubiofossil is proven can it be considered a true fossil; otherwise, it is classified as a pseudofossil resulting
from abiotic processes (Hofmann, 1972; Monroe and Dietrich, 1990; McMahon et al., 2021). To verify the origin of
dubiofossils, it is necessary to apply biogenicity criteria (Buick, 1990; McLoughlin and Grosch, 2015; Davies et al., 2016;
Neveu et al., 2018; McMahon et al., 2021; Rouillard et al., 2021).

As an emerging area of science, biogenicity criteria are arguments proposed to defend or refute the biotic origin of a given
65   object. As they depend on the type of material studied, they are multiple and can be grouped into four classes: 1) morphology,
structure, and texture; 2) relationship with the matrix or with inserted medium; 3) composition (including bioindicators); 4)
context (environment and age) and comparison with other similar biotic/abiotic objects (Buick, 1990; García-Ruiz et al., 2002;
Brasier et al. 2002; Schopf et al., 2002; Brasier et al., 2004; Westall 2008; Noffke, 2009, 2021; Slater, 2009; Wacey 2010;
Brasier and Wacey, 2012; Schopf and Kudryavtsev 2012; McLoughlin and Grosch 2015; Callefo et al. 2019a; Gomes et al.
70   2019; Neveu et al. 2018; McMahon et al. 2021; Rouillard et al. 2021). To refute the contamination hypothesis, it is important
to verify the indigeneity and syngenicity of proposed fossil (Rouillard et al., 2021). Additionally, comparing these materials
with abiotic and biotic objects can be essential for refining and defining their origins (Rouillard et al., 2021).

Through these investigation stages, dubiofossils had their origin improved and linked to biotic or abiotic processes. Biogenicity
criteria are better established for microfossil-like artifacts (Buick 1990; García-Ruiz et al. 2002; Brasier et al. 2002, 2004;
75   Schopf et al. 2002; Hofmann 2004; Schopf, 2006; Schopf et al., 2007; Schiffbauer et al. 2007; Schopf and Kudryavtsev 2012;
McLoughlin and Grosch 2015; Maldanis et al., 2020; McMahon et al. 2021; Rouillard et al. 2021; Martins et al., 2022);
followed by microbially induced sedimentary structures, stromatolites and ichnofossil-like objects (Noffke et al., 2001, 2002;
Westall and Folk, 2003; Porada et al., 2008; Noffke, 2009; 2021; Wacey 2010; Davies et al., 2016; Lerner and Lucas 2017;
Inglez et al., 2021). Nevertheless, these relatively well-established criteria can rarely be applied to other objects, like minerals,
80   lacking arguments to support biogenicity.

Minerals can be either biotic or abiotic and constitute the fundamental record of abiotic processes and one of the main records
of life activity over time. Due to the ubiquity of life forms in geological processes (from superficial processes to meso- and
telodiagenesis; Fig. 1) and to the existence of biomimetic inorganic minerals (Weiner and Dove, 2003; Weiner, 2008; Dupraz
et al., 2009; Bindeschedler et al., 2014; Bower et al. 2015; Tisato et al. 2015; Muscente et al., 2017; McMahon and Ivarsson
85   2019; Merino et al., 2019; Davies et al., 2020; Eymard et al., 2020; Suchý et al., 2021) it lacks arguments to differ purely
abiotic minerals from controlled, induced, and influenced biominerals (Dupraz et al., 2009). To improve the biogenicity
evidence for crystals is essential investigate mineral dubiofossils.

Recent investigations have focused on stick-shaped dubiofossils and alleged biominerals, leading to the development of some biogenicity criteria (Cailleau et al., 2009; Bindschedler et al., 2014; Tisato et al., 2015; Baucon et al., 2020; Green 2022).

90 However, due to the wide range of biominerals and biomimetic minerals (Dupraz et al., 2009), it is essential to examine more mineral dubiofossils and propose both biotic and abiotic evidence to strengthen these criteria. In this context, we present an example of a mineral dubiofossil from the Pennsylvanian age in Brazil.

The purpose of this study is to explore the origins of the multiple mineralized, elongated, ramified dubiofossils in question. Previously thought to be sponge spicules from the Pennsylvanian Paraná Basin, these elongated tubes will be examined across

95 four categories: 1) morphology, structure, and texture; 2) relationship with the matrix; 3) composition; and 4) context, including paleoenvironmental factors and biotic elements. Through additional analysis, we will diagnose the indigeneity and syngenicity of the material and compare it to both abiotic and biotic minerals in order to better understand its origins. We endeavor to unravel the intricate history of unique mineral occurrence, which has been shaped by the overlapping effects of geologic processes and the omnipresence of life. Through our efforts, we aim to shed some light on the interplay between biotic and

100 abiotic minerals. Ultimately, we propose this descriptive protocol that can facilitate investigations into dubiofossils.Suspendisse a elit ut leo pharetra cursus sed quis diam. Nullam dapibus, ante vitae congue egestas, sem ex semper orci, vel sodales sapien nibh sed lectus. Etiam vehicula lectus quis orci ultricies dapibus. In sit amet lorem egestas, pretium sem sed, tempus lorem.

1.1 Geological settings

105 Paraná Basin is an intracratonic Paleozoic-Mesozoic basin, covering an area of about 1.5 million square kilometers, extending across southern Brazil, Paraguay, Argentina, and Uruguay (Fig. 2; Milani et al., 2007). The Rio Ivaí, Paraná, and Gondwana I Supersequences (Milani et al., 2007) register the Paleozoic transgressive-regressive cycles with evolution linked to the stabilization of West Gondwana, the active Andean margin and the activity of the paleo-ocean Panthalassa. As well as the Supersequences Gondwana II and III deposited during the Mesozoic, whose continental sediments are associated with

110 extensional events and volcanic rocks linked to the fragmentation of the supercontinent Gondwana (Milani et al., 2007). Most of the basin's units belong to the Gondwana I Supersequence, a record of the transgressive-regressive cycle at the end of the Paleozoic-Triassic caused by the establishment of the greatest Phanerozoic ice age and its transgressive/climatic response (Milani et al., 2007). The Itararé Group record the effects of this glaciation (Valdez Buso et al., 2019).
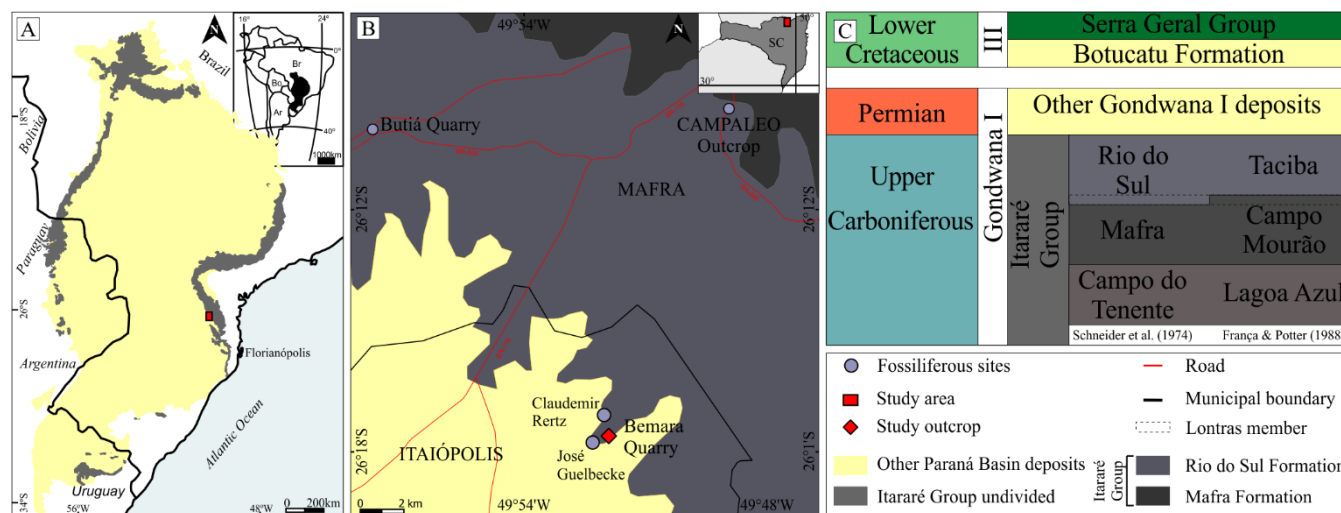
Figure 2: Location and geologic context of the collection area. A) coverage area of the Itararé Group in the Paraná Basin in south-central Brazil and neighbouring countries, study area; B) Location of the collection area, Bemara Quarry, municipality of Itaiópolis and other paleontological sites in the region, including similar to Bemara Claudemir Retz and José Guelbecke locations, geological units of study, Mafra Fm., Rio do Sul Fm. (Itararé Group) and other sequences of the Paraná Basin; C) Temporal distribution of the studied units, Itararé divisions based on Schneider et al. (1974) and França and Potter (1988). Based on Weinschütz and Castro (2006) and Valdez Buso et al. (2019).

115   The Itararé Group record the glaciogenic deposits of the Late Paleozoic Ice Age (LPIA – Isbell et al., 2003) as glacioterrestrial, glaciomarine and deglaciation successions of tillites, diamictites, sandstones, ritmites, and shales, that have lasted about 16 Ma, from the Bashkirian to the Gzhelian (Daemon and Quadros, 1970; Schneider et al., 1974; França and Potter, 1988; Souza, 2006; Cagliari et al., 2016, Valdez Buso et al., 2019; 2020). The Itararé group (Fig. 2c) is classified using field data by Schneider et al. (1974) in the Campo do Tenente, Mafra and Rio do Sul Formations and by França and Potter (1988), with

120   subsurface data, in the Lagoa Azul, Campo Mourão and Taciba Formations. These units are similar in lithology and time, except for the Lontras member which is the base of the Rio do Sul Formation and the top of the Campo Mourão Formation respectively. As the material was collected in outcrop, we prefer to use the first classification by Schneider et al. (1974).

In the study region (Fig. 2b), the Rio do Sul Formation crops out as sparse sandstones and a great abundance of diamictites and rhythmites, interpreted by Vesely and Assine (2006) of a distinct pattern of deglaciation, in which the turbidity currents

125   of melting had a less important role than the rains and resedimentation. Therefore, the regional interpretation corresponding to distal marine turbidites associated with delta systems caused by deglaciation final phase, corresponding to the upper part of the Itararé Group (Salamuni et al., 1966; Schneider et al., 1974; Canuto et al., 2001; Weinschütz and Castro, 2006; Puigdomenech et al., 2014; Aquino et al., 2016; Schemiko et al., 2019; Vesely et al., 2021). The Paraná Basin Paleozoic section is cut by sills and dikes of Serra Geral Group that fed the Large Igneous Province Paraná-Entendeka flows around 130 Ma

130   (Zalán et al., 1985; Almeida, 1987; Nardy et al., 2002; Frank et al., 2009). The detailed outcrop description with sedimentary structures and biotic elements is presented at the Sect. 3.1.4.

2 Material and methods

Samples were collected at Bemara quarry in Itaiópolis city (Santa Catarina State, Southern Brazil), approximately 12 km far from BR-116 Highway (km 29), geographical coordinates 26°17'44.5"S, 49°51'49.9"W (Fig. 2A and B). The Rio do Sul

135 Formation, topmost unit of the Itararé Group, Paraná Basin, crops out at this quarry. Approximately 250 siltstone and claystone slabs of different sizes with the structures were described and are kept in the fossil collection of Laboratório de Paleontologia of Universidade Federal de Santa Catarina (LABPaleo – UFSC).

To guarantee the total survey of the biotic and abiotic characteristics of the material in question, fulfilling the four attribute classes, the 250 hand samples were described and selected for more specific analyzes described below. To approach the (1)

140 morphology, structure, and texture and (2) relationship with the matrix, we used macroscopic description, petrographic microscopy, and X-ray computed microtomography. To describe (3) composition, in addition to the aforementioned techniques, we applied Scanning Electron Microscopy, with Energy Dispersive Spectrometry, X-Ray Diffractometry, and Raman Spectroscopy. To discuss the (4) context (paleoenvironment and biotic elements) and (5) indigeneity and syngenicity, we used field-collected data. Some ichnofossils were observed under a stereomicroscope in the laboratory.

145 ### 2.1 Macroscopic description and petrographic microscopy

The specimens were characterized in an Olympus SZ51 stereomicroscope and measured by an analogic caliper. Different morphologies were described. Length, width, and relative angles of the branches were measured. Eight thin-sections, one perpendicular, and seven others concordant to the bedding plane were characterized in a Zeiss petrographic microscope at Laboratório de Geoquímica of Universidade Federal de Santa Catarina (LABGeoq – UFSC) and a Zeiss Stemi 305 at

150 Universidade do Vale do Rio dos Sinos (UNISINOS), using 2.5, 10, 25 X objective lenses.

2.2 X-ray computed microtomography (Micro-CT)

One sample was analyzed for three-dimensional structure and architecture using a Zeiss/XRadia Versa-500 micro tomograph at Laboratório de Meios Porosos e Propriedades Termofísicas of Universidade Federal de Santa Catarina (LMPT – UFSC). This equipment operates from 30 to 160 kV energy range, with power up to 10 W. Treated in FIJI open software

155 (https://imagej.net/software/fiji/).

2.3 Scanning electron microscopy (SEM) and energy dispersive spectrometry (EDS)

Three hand samples and one thin section were selected for SEM-EDS analysis at Instituto Tecnológico de Paleoceanografia e Mudanças Climáticas (ITT OCEANEON – UNISINOS) using an EVO/MA15 Zeiss scanning electron microscope. They were metalized with 46 nm of gold. Tension ranged between 15-20 kV with five interactions.

2.4 X-ray Diffractometry (XRD)

A siltstone slab, containing at the same level a portion with distributed elongated material and the other only with matrix, was prepared for the mineralogical XRD analysis. Two rock powder samples (one with the dubiofossil under study) were dried in an oven at 40°C for two hours, recovered, mounted in sample holders by the back-loading method, and taken to the diffractometer. XRD was performed at ITT OCEANEON – UNISINOS using an Empyrea PANanalytical, with reflection-transmission and spinner set at two revolutions per second, goniometric range from 2 to 75° (2θ), with a step of 0.01 for 330s, Cu tube (CuKα), and at 40 kV and 40 mA.

2.5 Raman Spectroscopy (RS)

One horizontal thin-section was analyzed for mineralogical characterization using a Micro-Raman Renishaw, at Laboratório de Astrobiologia of Universidade de São Paulo (AstroLab – USP), using 5x and 50x lenses and laser 785 nm, potency between 5 and 10%, with at least 30 acquisitions, capturing specters of the first order (150 to 1350 cm-1) and second order (1250 to 2250 cm-1) ranges. The obtained 16 first order, and 11 second-order point signs (stacked specters), and two compositional mappings were treated on WiRE 4.4 and OrigingPro8.

3 Results and Discussion

3.1 Description

3.1.1 Morphology, structure, and texture

The structures vary in size, shape, and packing, although there is a general stick-shaped (needle-like shape) of whitish material (Fig. 3). Size varies strongly between 0.04 and 16 mm in length and between 0.01 and 1.5 mm in thickness, with constant thickness within each stick. The packing can be loose or dispersed (Fig. 3), distributed freely concordantly in the matrix layer as a random texture, continuously covering the sample as a 2D pavement (Fig. 3A and B), or ending with increased packing in straight or curved contours (Fig. 3C and D). Thus, geometry ranges from simple to complex. The sticks appear as 3D tubules, flattened tubules, molds, and impressions, mainly straight, but there are some curved and sinuous (Fig. 3E-I). Some 3D forms have a dark tubule inside the white layer (Fig. 3F), while others have a fainter white outer layer (Fig. 3G). In Micro-CT, the stick is distinct from the matrix as a denser tube with a less dense central tube (Fig. 6), with true ramification and circular cross-section (Fig. 6F-G). The most common structures are small unbranched sticks (Fig. 3D) and the second are elongated rods with multiple random short branches (Fig. 3F) there are also radial forms and little dots (Fig. 3E). Usually, one morphotype dominates each fine-grained slab, related to the matrix composition. Due to the spectrum of shapes, we propose four informal

classes (Fig. 4 and Table 1): A) unramified rods in light gray siltstone; B) ramified elongated forms in black to dark gray siltstone; C) large radial forms in black mudstone; D) unramified sticks with some ramified tubules and dots in dark to light gray siltstone.

190 Class A (Fig. 4A and B) present a random texture of straight small rods, length of 0.04 to 10 mm (mean 2.5 mm, standard deviation 1.9, Table 1), most of them with a 3D shape with well-defined limits in yellowish white material, that can have a
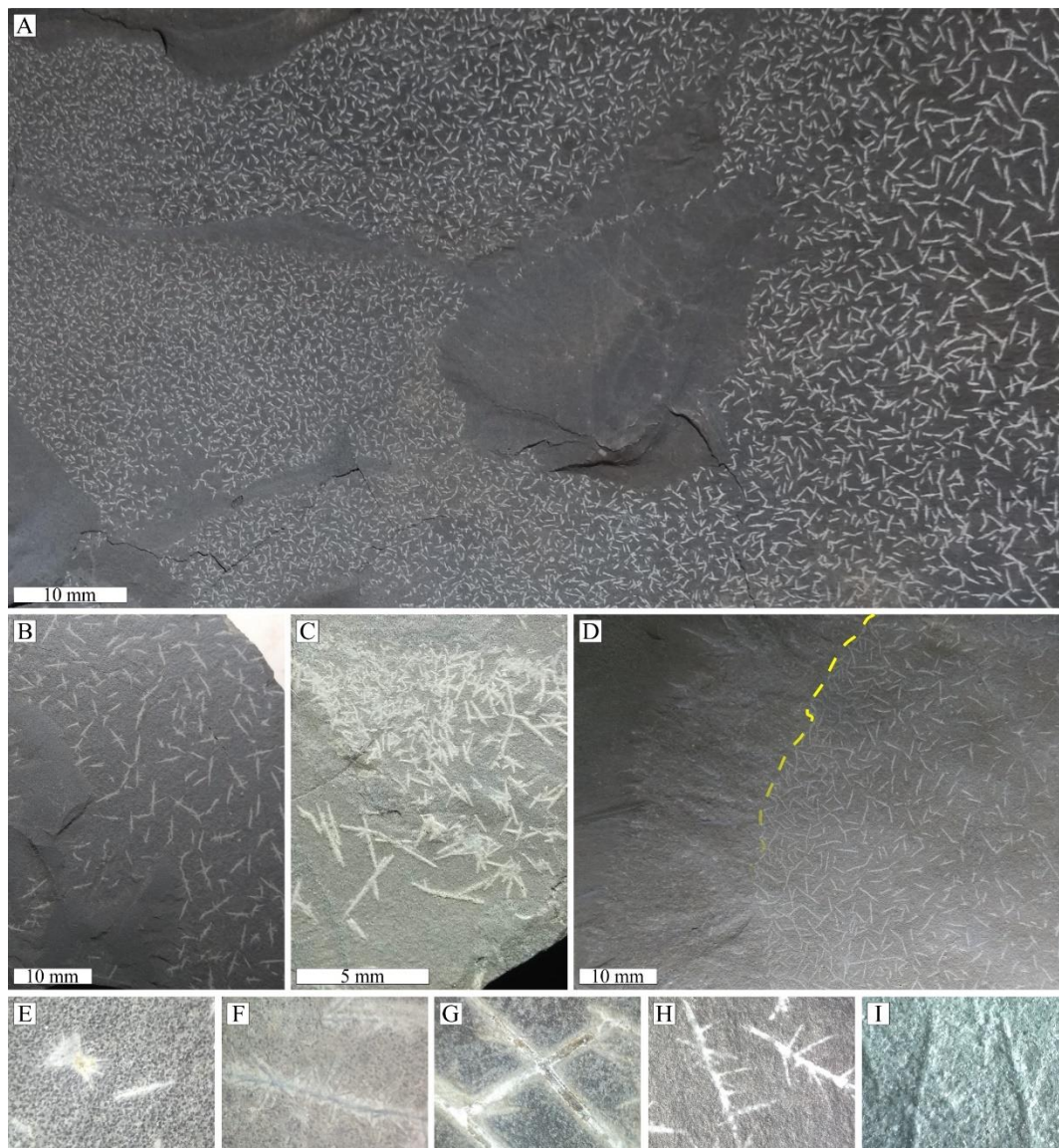
Figure 3: General distribution and morphology of dubiofossils: A) 2D pavement of concordantly loose sticks; B) Dispersed ramified sticks; C) increased packed of sticks in straight contours; C) increased packed of sticks in curved contours; E) non-ramified sticks and radial forms; F) elongated ramified 3D sticks, with dark central axis; G) flattened sticks, with a dark central axis and fainter external layers; H) 2D white lateral ramified sticks; I) Mold of the slightly curved sticks.

secondary pale white cover (Fig. 4B). Both ends are better preserved and gradually taper to the tip (some can have spindle shape), the central area can have a dark axis or be completely faded. The black interior tubule is also recognized when the sticks are broken longitudinally, presenting a circular transversal section. Longer than class A, the class B ramified elongate structures (Fig. 4C and D) can be straight or sinuous. In class B, length varies from 0.05 to 14 mm (mean 3 mm, sd 2.1; Table 1), and is variable between the main axis and the branches. The 3D structures are dark gray (Fig. 4C), showing occasionally a faded white margin, while the 2D are white well-defined impressions (Fig. 3H). Most structures have many primary short ramifications, that do not show a periodicity of spacing or a trend of direction, or a regular angle with the main axis (ranging from 25° to 90° concerning the axis). Most of the branches depart from the main axis, but there are often branches emerging to both sides, crossing the feature (Fig. 4D). Secondary, there are sticks that ramify at only one end, separating into three or four points and others with four tips forming irregular crosses. Punctually, there are sinuous structures with long primary branches and short secondary branches, also in aleatory directions.

205
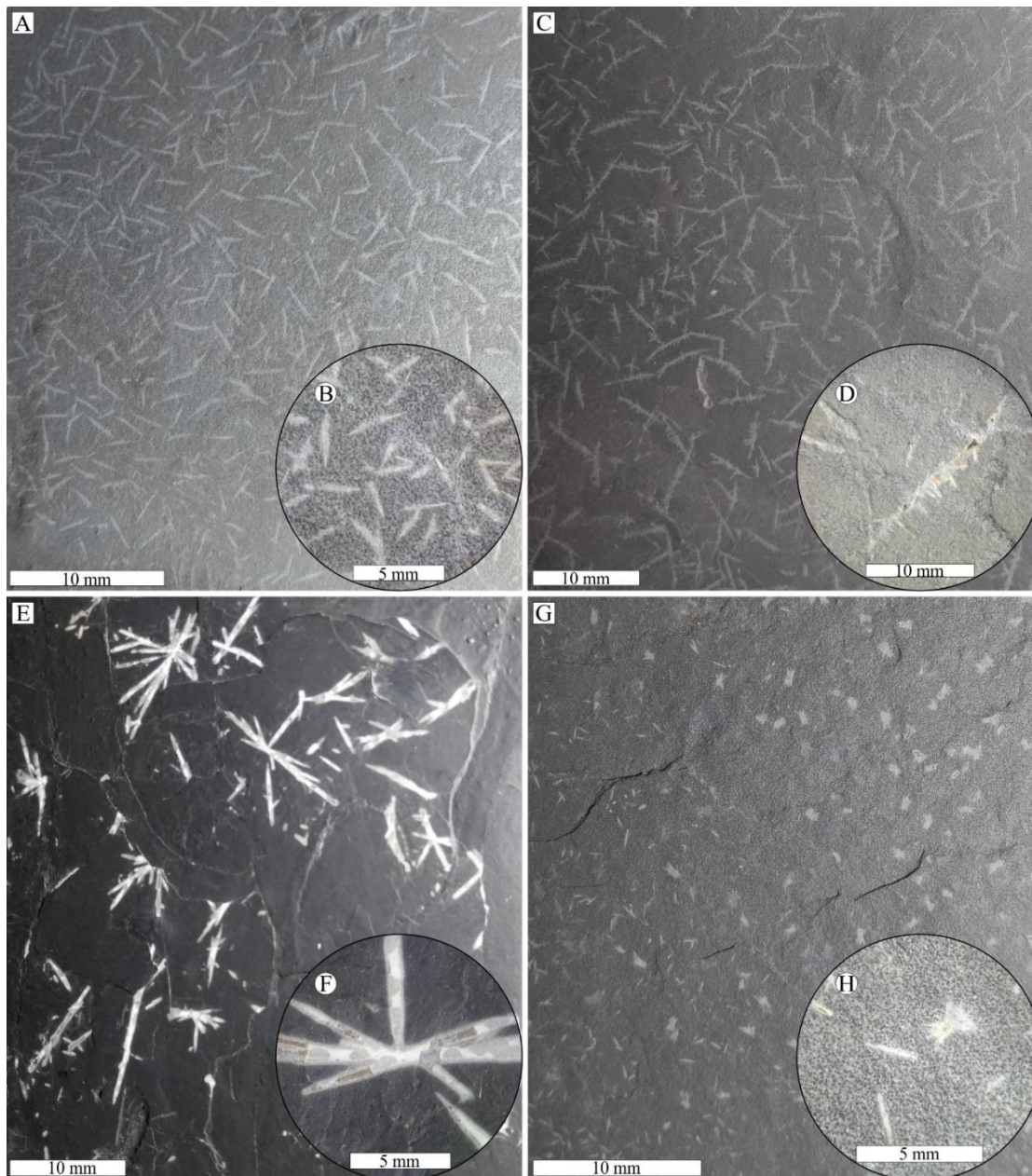
Figure 4: Informal classes of dubiofossil forms related to the matrix: A) General view of class A, loose packed unramified sticks; B) closed-up view of class A yellowish-white sticks with tapered tips and fainter regions; C) General view of class B, laterally ramified sticks; D) example of class B ramified sticks, branches depart from and crossing the main axis; E) General view of class C, radially ramified dubiofóssil; F) Detail of class C radially ramified structures, with tapered tips, external fainter layer, and internal dark layer; G) General view of class D, small sticks and dots, each dominating one side of the slab; H) Closed up view of class D non ramified sticks and "dots", small radially ramified forms.

Class C and D are rarer. Class C seems linked to the darker matrix, presenting dispersed radial structures as impressions or flattened rods (Fig. 4E and F). The well-defined branches are of white material with straight walls (length 3 to 16 mm, mean 4.1, sd 3; Table 1), and the angles with the apparent central line have no pattern or periodicity (varying from 11° to 86°). The thickness and length of the branches are variable, as well as the tips, when present, gradually taper towards the end. Moreover,

210 in the direction of the center, they also seem to taper (Fig. 4F). The class D (Fig. 4G and H) is composed of unbranched or little branched rods associated with dot structures that appear to be small radial features (0.013 to 1 mm), ramification angles vary from 9° to 86° (Table 1). Typically, one of these structures dominates one side of the plate, showing a transition of shape dominance (Fig. 4G). The sticks are in 3D and 2D white material with different degrees of alteration, similar to class A, with lengths of 1 to 10 mm. In general, classes B, C, and D present a greater variation in size, as well as greater diversity in formats

215 than class A.

Table 1: Informal classes of dubiofossil morphology related to the associated matrix, mode of occurrence, length, and branching angles.

Class	Morphology	Associated matrix	Mode of preservation	Length (mm)	Main axes angles
A	Non-ramified straight	Light gray siltstone	3D white tubes with dark core faded border present or not, molds and 2D impressions	0.04 to 10 (mean 2.5, sd 1.9)	–
B	Laterally ramified	Black to dark gray siltstone	3D black tubes and white tubes, faded border present or not 2D white impressions	0.05 to 14 (mean 3, sd 2.1)	25° to 90°
C	Radially ramified	Black mudstone	White 2D impressions or 3D flattened tubules	3 to 16 (mean 4.1, sd 3)	11° to 86°
D	Little branched needles associated with dots	Dark to light gray siltstone	2D impressions, molds and 3D white tubes with dark core faded border present or not	Acicula: 1 to 10 Dots: 0.013 to 1	9° to 86°

On petrographic thin section, the sticks are euhedral to subhedral, colorless, low relief, without twins or cleavage (Fig. 5). It

220 may have a black opaque central axis in the elongation direction and, less commonly, an opaque brownish outer edge (Fig. 5A-C). The rod material has a microgranular texture with 1st to 2nd-order birefringence, with incomplete extinction that appears mottled and oblique (Fig. 5C and D; G-H). In longer rods, undulating extinction is common, without the main orientation. On more altered sticks, the external faded edge appears as an irregular gray texture never extinct. The class B longer rods show a higher degree of crystallization, with the 1st-order nanocrystalline graduating to the 2nd-order

225 microcrystalline towards the center (Fig. 5d). As for class C, structures can have the central opaque axis or two axes around

the crystalline material. In general, the sticks show irregular layers in the direction of the central axis of microporous texture intercalated with smooth or microgranular texture (Fig. 5C), sometimes aligned subspherical blocks (Fig. 5F).
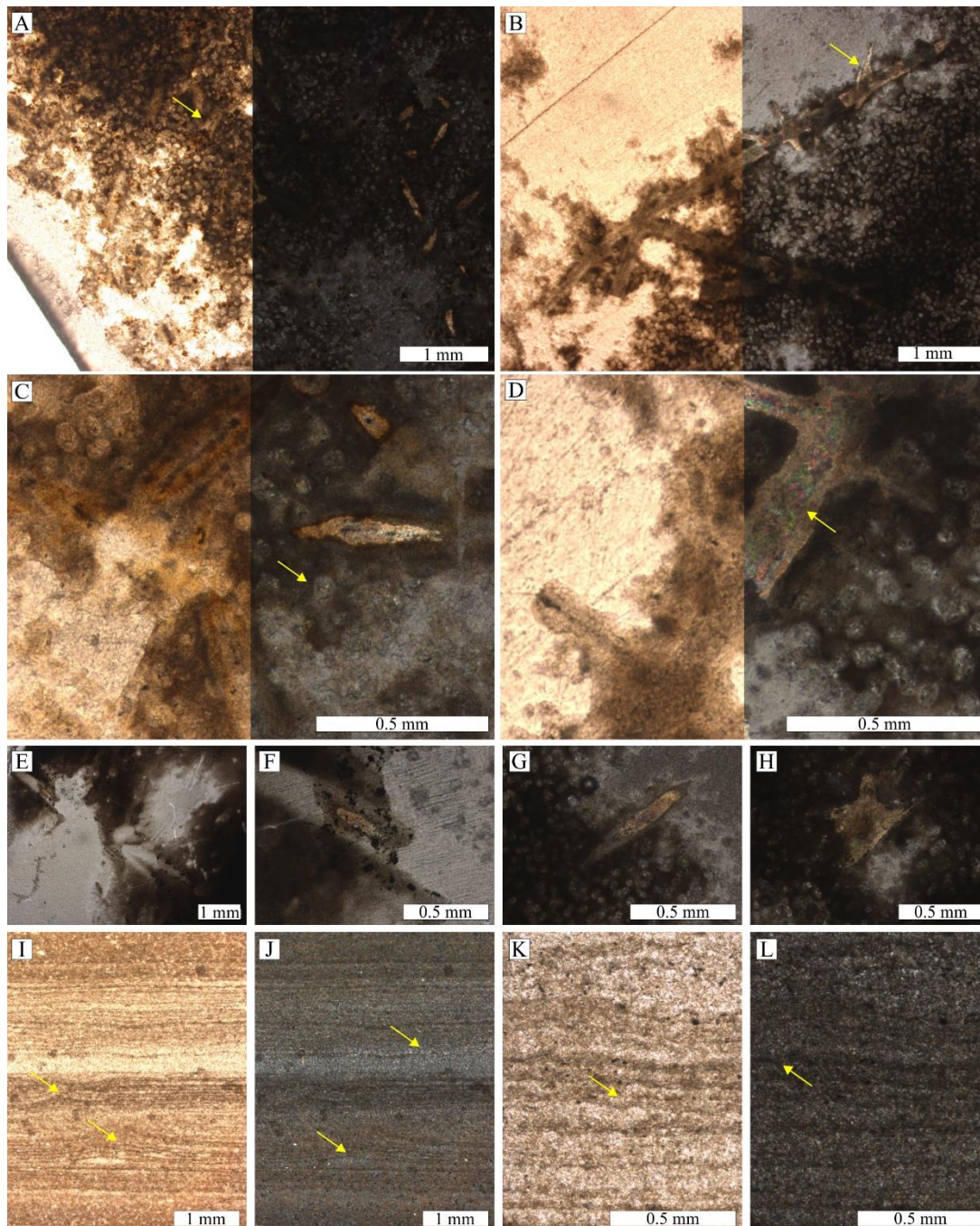
Figure 5 Figure 5: Petrographic thin-sections: A) Class A sticks (arrow) distributed with the spheres inside the matrix, left natural light, right: polarized light, sticks in higher birefringence; B) Class B ramified stick with the spheres inside the matrix, left, natural light, right, polarized light, dubiofossil in higher birefringence, arrow pointed to a dark main axis in a branch; C) Close view of class A sticks with main dark axis, white layer, brown layer and a second white layer, left, natural light, right, polarized light, dubiofossil in higher birefringence, arrow pointed to a matrix sphere; D) Close view of class B stick, , left, natural light, right, polarized light, arrow pointed to the microcrystalline texture with higher birefringence (corresponding to the white layer), with nanocrystalline externally; E) Close view of class C radially ramified mold, polarized light; E) Close view of class C, internal composition partially preserved with second order birefringence, polarized light; G-H) Close view of stick and radially ramified structures of class D, polarized light. I-L) Microfabric of the matrix in vertical thin-section, well-laminated, undulated, and disrupted lamina (arrows) related to sinusoidal and laminated leveling microstructures. I-K, natural light; J-L, polarized light.

3.1.2 Relationship with the matrix

230   The sticks are embedded in the matrix composed of an agglomerate of circular/subcircular transparent forms and brown opaque cement. The subspherical shape is attested in the vertical thin-section and Micro-CT (Fig. 5 and 6). Some look to be joined and aligned in groups of 2 to 6 spheres, forming ellipses and straight to sinuous lines with a globose limit (length up to 0.5 mm). Each circle has a low birefringence and is never extinct (Fig. 5C and D), with the diameter ranging from 0.04 to 0.1 mm. Some show a central black point or are polyhedric with subhedral faces delimited by brown lines. The sticks are inserted in

235   the lamina, always horizontal, as demonstrated by Micro-CT (Fig. 6), never cross or disarray the matrix spheres, and both are covered by brown cement (Fig. 5 and 6). Despite similar microstructures, central or wall, dubiofossils are distinguished from matrix spheres by size, degree of crystallinity, and higher birefringence, there is greater morphological complexity, more layers, and branching (Fig. 5).

240
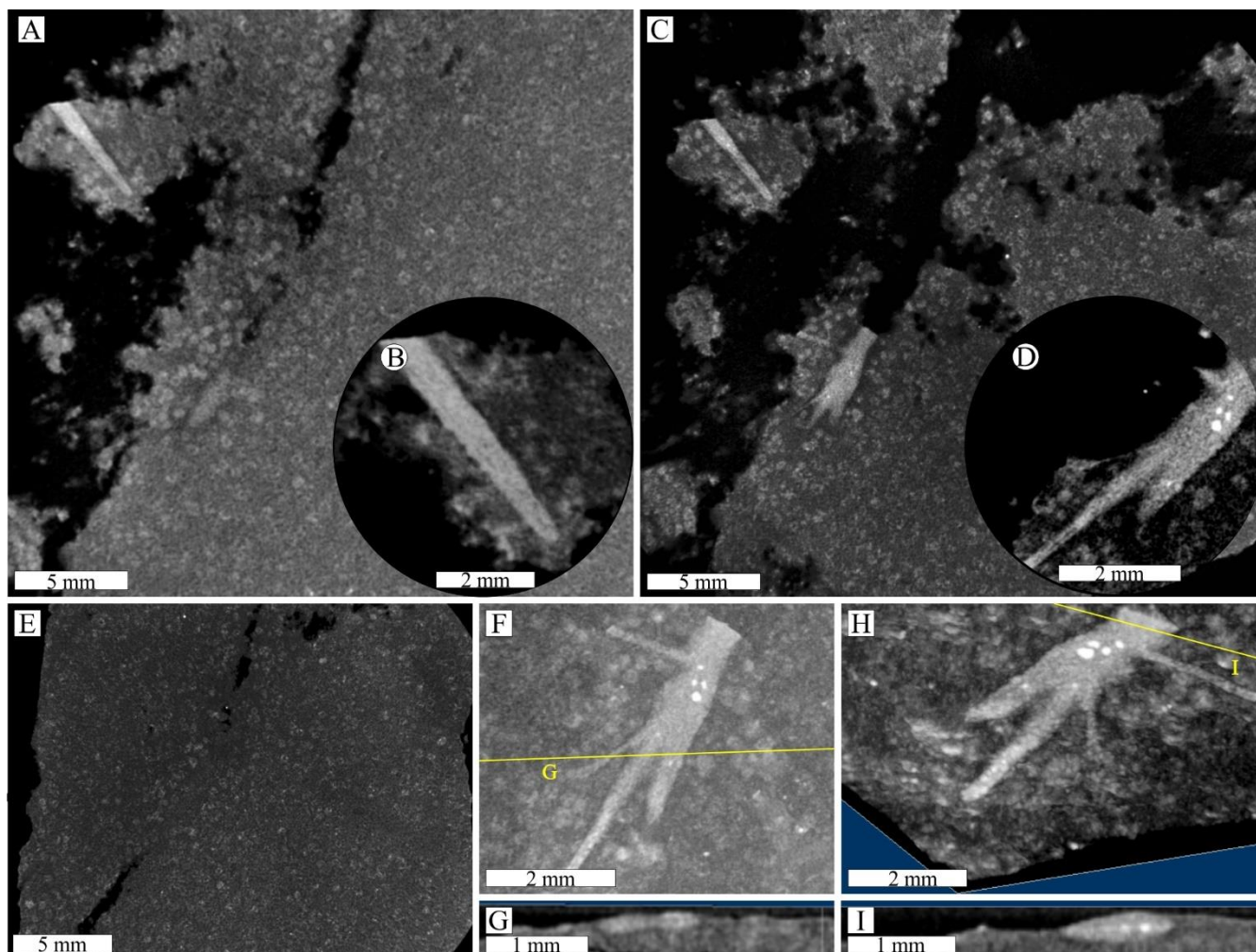
Figure 6: Micro-CT results, sticks (lighter gray structure), matrix (darker gray), and matrix spheres (gray circles): A) General view of a non-ramified stick; B) close view showing the internal structure (slight density differences inside the tube); C) View of ramified structure; D) Close view of the ramified tubule, middle tubule less dense. E) Matrix view with multiple matrix spheres. F-H) Cross-section demonstrating the true ramification and insertion in the matrix.

3.1.3 Composition

The composition corroborates the difference between the elongated structures and the matrix. The matrix EDS shows an expected composition for siliciclastic muds and silts of O, Mg, Al, Si, K, and Fe (Fig. 7E). While the sticks exhibit a complex element distribution following the pattern of texture described above (Fig. 7D and E). The main dark axis has O, Mg, Al, and Fe composition. The first layer (crystalline white/yellowish white) is dominated only by calcium and depleted on other elements. The second layer seems similar to the main axis presenting a brown or dark appearance in which O, Mg, Al, and Fe occur. Another external layer irregular gray texture, not always present, have O, Na, Al, Si, and K composition. C, Mn, and S appear weakly dispersed throughout the material, while Ti and sometimes S are concentrated in spots in the matrix and sticks

(Fig. 7F). Although Mg, Al, Si, K, and Fe cover the whole matrix, sometimes Mg and Fe appear concentrated in the matrix
250   spheres and Al and Si seem less concentrated in the same areas (Fig. 7E).
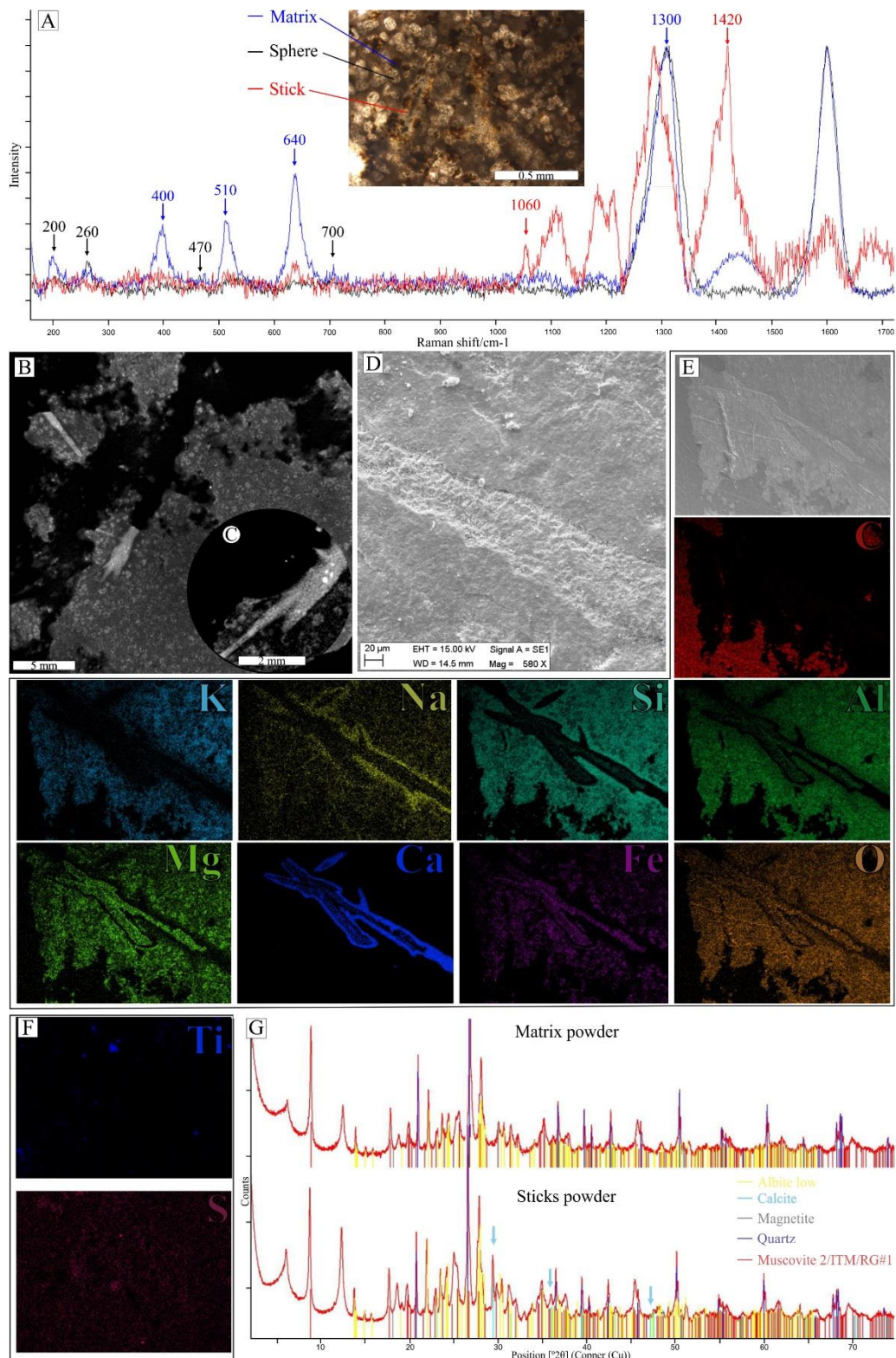
Figure 7: Paleometric results: A) Raman specters of the thin section, matrix, blue sign, with hematite peaks (~400, 510, 640, and 1300 cm-1); spheres, black sign, with clay mineral composition (~200, 2060, 470 and 700 cm-1) and stick, red sign, with carbonate peaks (~1060 and 1420 cm-1); B-C) Density differences between matrix (dark gray), spheres (gray) and sticks (light gray); D-F) SEM-EDS results: D) Secondary electron image of part of the stick in hand sample, different textures of the matrix, margin, and center of the stick; E) Backscatter electron image and EDS composition of a ramified stick in thin-section, C, K, Na, Si, Al, Mg, Ca, Fe, O detected in different distributions; F) EDS results of dispersed S and points of Ti in the matrix, other sample measured; G) Graphical signs of XRD powder analysis, matrix without (upper) with (lower) sticks, the difference in the peaks of calcite present in the sticks (blue arrows).

Between classes (A, B, and C), there was no difference in elemental composition, which varies, in addition to the external shape and crystallinity described above, in coverage and the compositional sequence. As class A is composed of smaller sticks, it had a smaller coverage of Ca and Fe layers, with central axes (Mg, Al, K, and Fe) better defined. Class B is organized

255 similarly with relatively greater coverage of Ca. Class C appears a little more distinct with less calcium coverage, a wider central axis of O, Mg, Al, and Fe with a higher iron concentration towards the edges before the calcium wall.

The mineralogical composition agrees with the EDS elemental data. The brown amorphous material in the matrix contains hematite (as measured by Raman spectroscopy, peaks 400, 510, and 640 cm^{-1} and XRD; Fig 7A and G) and possibly magnetite (captured by XRD, Table 2), organic matter not encountered in RS or XRD. The spheres are probably clay minerals/micas,

260 measured by RS (Fig. 7A, peaks of 200, 260, 470, and 700 cm^{-1}) and corroborated by XRD (undefined clay minerals 14 Å and 7 Å). The XRD also indicated the presence of quartz, biotite, and albite. As in the EDS, the sticks have a different composition, the RS peaks at 1060 and 1420 cm^{-1}, were interpreted as possible disordered carbonate minerals due to deviation and formation of additional peaks, which makes it hard to characterize the material (Fig. 7A). Calcite inferred by XRD, present only in the powder sample that contained the sticks (Fig. 7G and Table 2).

265

Table 2: XRD powder results with and without sticks

Matrix with sticks	Only matrix
Quartz	Quartz
Calcite	
Muscovite	Muscovite
Albite	Albite
Magnetite	Magnetite
Clay mineral 14 Å	Clay mineral 14 Å
Clay mineral 7 Å	Clay mineral 7 Å

Therefore, by the distribution of the elements in the sticks, corroborated by RS and EDS, it is possible to infer a dolomite/ankerite composition in the central area and a calcitic to surrounding layer, whose main dark axis concentrates O, Al, Mg and Fe and the whiter layers concentrate calcium. The external brown layers of O, Al, Mg, and Fe are considered clayey

270   cement in the matrix, and the outermost layers are interpreted as a recent alteration of the material from clays rich in Na and

K.

3.1.4 Context, paleoenvironment and associated biotic elements

The outcrop exhibits 14 m of heterolith (Fig. 8A) defined by tabular centimetric layers (0.2 to 4 cm) of normally graded
siltstones, rhythmically alternated with black mudstones, which are usually massive or present sub-millimetric lamination.

275   There is a thinning-upward tendency with the predominance of sand layers at the base and mud layers at the top (Fig. 8A).
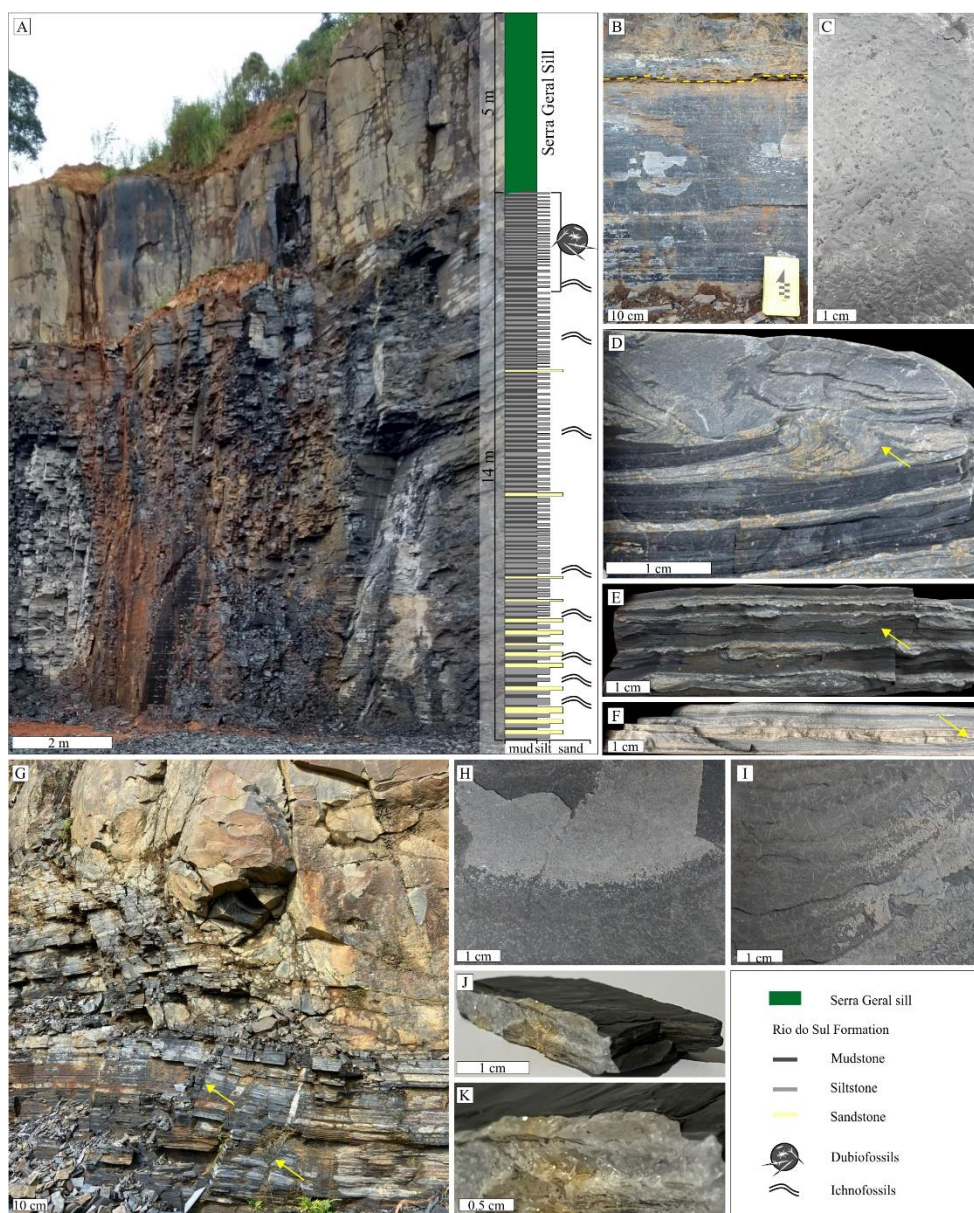
Figure 8: Local geologic features. A) Bemara Quarry, a section of 14 meters of heteroliths enclosed by the sill of the Serra Geral Group, a schematic section of the lithological distribution and presence of ichnofossils and the dubiofossil under study; B) Occurrence section of the dubiofossils in the heterolith, close to the contact with the sill (dashed line); C) Pseudonodules on the mudstone slab, seen in plain view; D) Flames and syndepositional folds (arrow); E) flute cast and syndepositional charge structures (arrow), cross-sectional view; F) sand layer with silt/clay load structures (arrow), cross-sectional view. G) Irregular contact between Paleozoic section and cretaceous sill, fractured zone (arrows); H) Horizontal quartz vein covering the silt layer with the sticks; I) Horizontal quartz vein partially covering flattened ripples with sticks; J) Vertical quartz vein cutting the siltstone and mudstone layers; K) Detail of the vertical quartz vein presenting the euhedral quartz crystals and brown cement.

Very fine to fine-grained sandstone layers with ripples are rare. Erosive structures such as sole marks, tool marks, flute casts, bounce, grooves, flames, and pseudo-nodules are frequent (8 C-F). Few dispersed granule clasts disturb the mudstone laminations, while erosive bases occur in sandstones.

Horizontal trace fossils and microbially induced sedimentary structures (MISS) are distributed throughout the section, present in different silty and muddy layers and became rare towards the top (Fig. 8A). Both fossil elements are widely investigated in other outcrops of the Itararé Group (Balistieri et al., 2002, 2003, 2021; Buatois et al., 2006; Gandini et al., 2007; Netto et al., 2009, 2021; Lima et al., 2015, 2017; Noll and Netto, 2018; Callefo et al., 2019b; De Barros et al., 2021) and help to understand the depositional environment.

As systematic ichnology is not one of our aims, here we present a brief description and identification of ichnotaxons. Simple shallow borrows *Helminthoidichnites tenuis* and *Treptichnus pollardi* are very common in the Bemara outcrop, as well as others in the Itararé Group (see Balistieri et al., 2021). The first, *H. tenuis*, appears in concave hyporelief on muddy and silty facies (some associated with the rods, Fig. 9E), with a curved to meandering shape and many crosses between specimens, identified as non-specialized grazing traces, produced by arthropod larvae or a worm-like animal in non-marine settings. The former, *T. pollardi*, appears as concave or convex epirelief of straight to curvilinear segments joined by small round pits, interpreted as a feeding trace probably produced by wormlike animals also in subaqueous non-marine conditions. In addition, there are slightly curved to straight shallow bilobed intrastratal structures, ornamented by fine striations arranged obliquely to the median groove, preserved by convex hyporelief, diagnosed as *Cruziana problematica* and *Cruziana* isp., interpreted as a product of arthropod locomotion into the substrate (Fig. 9B and F). Epistratal structures were recognized: there are sinuous and straight trails of *Diplopodichnus biformis*, composed of two parallel grooves separated by a median ridge, which may or may not be ornamented with podial imprints, preserved as concave epirelief, possibly produced by millipedes on a soft-ground substrate (Fig. 9A); Straight to strongly curved trackways consist of two parallel rows of podal impressions, without series, preserved as convex epirelief, recognized as *Diplichnites gouldi¸* also produced by millipedes on a stiff-ground substrate (Fig. 9A); As well as arthropod resting impression like *Gluckstadella* isp. This suite can be interpreted as Mermia-Scoyenia ichnofacies, palimpsest already diagnosed in other Itararé localities (Netto et al., 2009; Balistieri et al., 2021).
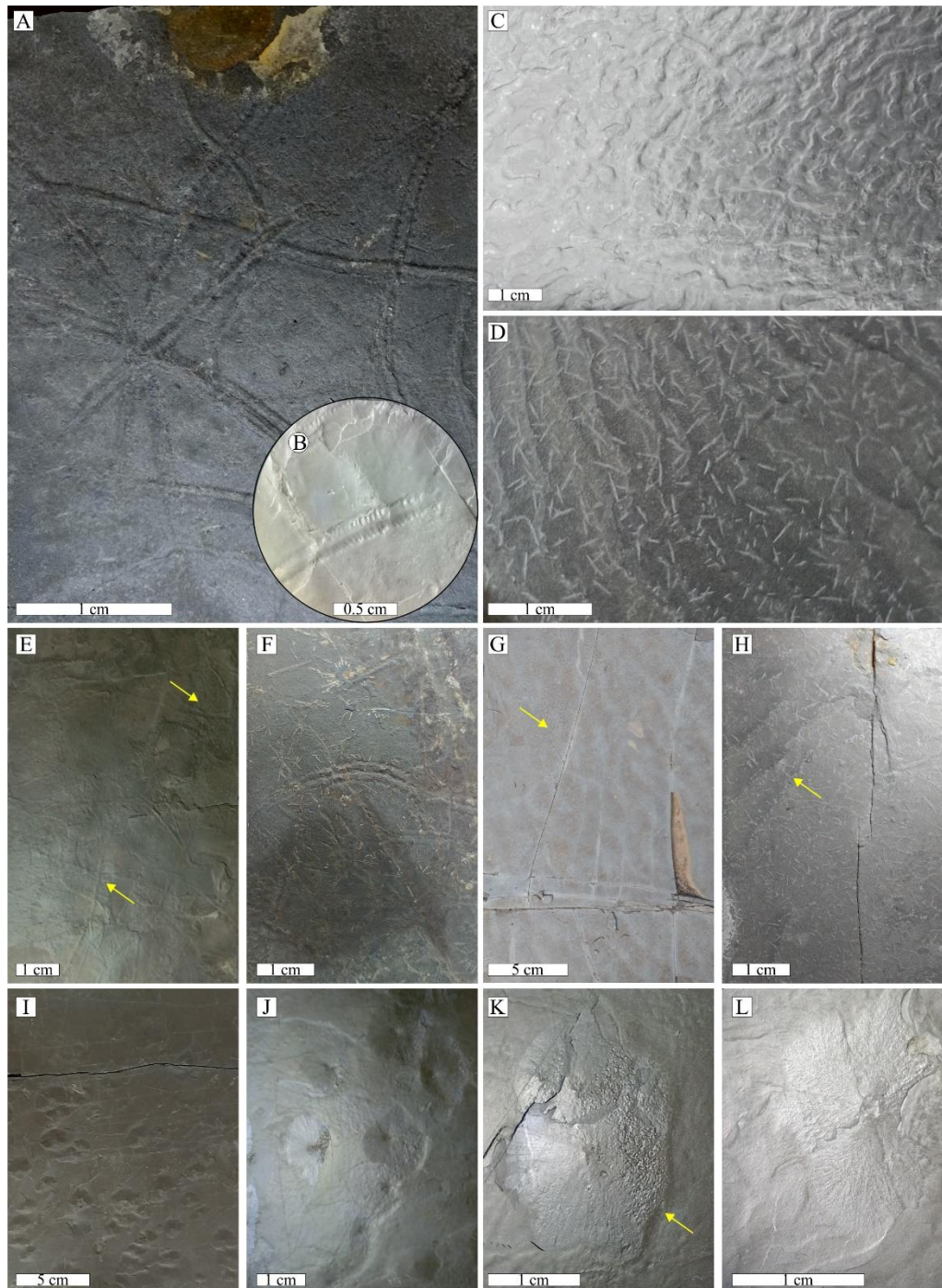
Figure 9: Associated biotic elements: A, B E and F Ichnofossils, C, D, G, H wrinkle structures and microbial mat elements, I-L small discs in the mudstones: A) *Diplichnites gouldi* **and** *Diplopodichnus biformis***; B)** *Cruziana problematica* **C) Kinneyia wrinkle structures, D) Flattened unidirectional ripples with sticks; E) Helminthoidichnites** *tenuis* **(arrows); F)** *Cruziana* **isp. at the center and** *Cruziana problematica* **at the top with the sticks; G) Multidirected ripple marks with sticks (arrow); H) Flattened ripples with sticks aligned in parallel clusters; I) counted slab with many cones; J) aligned discs; K) cone with flower form and vitreous luster and one side micro-wrinkle (arrow); L) Detail of the disc with a flat top.**

MISS are widely distributed in the Bemara quarry (Fig. 8A). Principally flattened unidirectional ripples with slightly sinuous parallel ridges (wavelength: 5 to 30 mm), occurring in several muddy and silty layers throughout the outcrop, including those associated with the sticks (Fig. 8I, 9D and H), presenting laminated leveling structures, the most common feature related to

305 the microbial mat at the study area. The dubiofossils are distributed following the morphology of the ripples or are concentrated in the trough forming parallel clusters (Fig. 9H). Wrinkle structures are irregular parallel to subparallel crests or very sinuous ridges (Kinneyia; Fig. 9C) that form a wrinkled pavement of claystone layers, typically non-transparent wrinkles. In addition, there are clusters of wrinkles type Arumberia (delicate subparallel lines) and elephant skin (fine corrugations). Besides, some levels present multi-directed ripple marks (Fig. 9G).

310 The microfabric seen in the vertical thin section corroborates with the macroscopic structures related to microbial mats. Despite not having layers composed of sand, hampering the visualization of oriented grains, the alternating laminar layers of silt and clay present a characteristic micro fabric, undulated and disruptive features related to sinoidal and laminated leveling microstructures (Fig. 5I-J). In addition, the microfabric contains mat layer-bound small grains (spheres, clays detected in XRD and RS) and possibly heavy minerals (opaque minerals and hematite detected in RS; Fig. 7A). The gradual alternation of dark

315 and light layers may be related to micro sequences, defined by Noffke et al., (1997) and Noffke (2010), and presented for other Itararé locality by Noll and Netto (2018) and Callefo et al. (2019b).

Some black argillaceous levels have clusters of small radial cones (1-4 mm in high and diameter ranging from 2 to 23 mm, with the mean of the largest and smallest diameter, 15.1 and 8.3 mm respectively) with a straight top of circular to subangular shape (maximum of 3 mm), whose sides are formed by radial lines or elevations (Fig. 9I-L). A vitreous luster distinguishes

320 them from the matrix with lobed edges that resemble a flower. In a slab measuring 1200 cm2, 157 objects were counted, most are aligned and elongated in one direction, sometimes with two or three discs joined (Fig. 9J), and normally one of the faces orthogonal to this alignment presents a micro-wrinkle (Fig. 9K). In the vertical section, a central tube is not observable, and the same massive texture occurs inside and outside the discs. Likely related to gas dome products of microbial metabolism (See Noffke, 2010 and Inglez et al., 2021).

325 All the features described favor the interpretation of extensive microbial mats throughout the Bemara outcrop, suggesting the presence of epibenthic communities, and possibly endobenthic, in a transitional lower supratidal to the upper intertidal environment (see Noffke, 2010, 2018 and references therein). The association between microbial mats and trace fossils is common in the rhythmic deposits of the Itararé Group (see Lima et al., 2015, 2017; Noll and Netto, 2018 and Callefo et al., 2019b) and reveals the colonization of the bottom of shallow water bodies by microbial mats and animals. The mats favored

330 the preservation and served as a food substrate for undermat miners (*H. tenuis* and *T. pollardi*) and overmat grazers (myriapods traces of *D. biformis* and *Gluckstadella* isp.) (see Lima et al., 2015).

The stratigraphic data corroborate the regional interpretation of large turbiditic systems related to melt discharges. The dominance of clayey and silty layers and deformations favor the interpretation of distal turbidites (regional interpretation by Weinschütz and Castro, 2006; Aquino et al., 2016; Schemiko et al., 2019; Vesely et al., 2021). On the other hand, the extensive

335 MISS and Mermia-Scoyenia ichnofacies are interpreted as shallow freshwater lakes, in near marginal marine settings, tidally

influenced (lower supratidal) intensively colonized by microbial mats and trace fossil producers, these environments quickly dried up or reduced the water column, evidenced by the dominance of myriapods (other locations interpreted by Balistieri et al., 2002, 2003, 2021; Netto et al., 2009; Lima et al., 2015; Noll and Netto, 2018 and Callefo et al., 2019b). Nevertheless, both interpretations are not conflicting. It is possible to associate the abiotic features on a larger scale, in which large cycles of

340 melting ice were deposited in turbidity flows, on a smaller scale, shallowing cycles caused by the rapid drying common in periglacial environments allowed the proliferation of the described biota. Due to the lack of stratigraphic detail positioning biotic and abiotic structures, it is not possible to clarify the frequency of these cycles in the outcrop, despite being present in units LPIA-related (Birgenheier et al., 2009). The patterns of decreasing towards the top of Bemara section in the abundance of fossil traces and sand layers reinforce this interpretation, as the sand indicates proximal portions of the turbiditic sequence

345 and therefore a shallow water column that favors evaporation and the establishment of this biota.

The outcrop is closed at the top by a diabase sill with irregular contact (approximately 5 meters; Fig. 8A, B and G), related to the Lower Cretaceous intrusions of Serra Geral Group (Silva, 2020), in which the last 3 cm of the sedimentary package close to the contact have a much higher hardness than the rest of the unit. The dubiofossils were collected in the last ~2 m of the top of the outcrop, close to this diabase sill (Fig. 8). Problematic features found in some, but not all, silt/mud layers, dispersed as

350 abundant concordant macrotextures and clusters, sometimes associated with trace fossils and MISS described above. The systematic collection showed an increase in dubiofossil layers towards the top, with the highest abundance between 50 and 20 cm below the sill contact.

The sill facilitates the correlation of the Bemara outcrop with two other very close ones, Claudemir Rertz and José Guelbeck, which have the same Paleozoic succession (sedimentary structures and biotic elements) and the same occurrence of

355 dubiofossils close to contact. In the José Guelbeck outcrop, approximately 600 m from the study point, Silva (2020) attested a halo of thermal effect, measured in palynomorphs from the sill contact up to 2.5 meters below and a zone of intense thermal influence > 50 cm (gray phytoclasts tied). In the Bemara outcrop, a similar thermal effect can be interpreted by an increase in the hardness of the Rio do Sul Formation laminae as it approaches contact.

Furthermore, the study area is cut by several vertical and subvertical fractures, some of them filled with whitish crystals that

360 are linked to the placement of the Cretaceous intrusive rock (Fig. 8G-K). This filling is different from dubiofossils because, in addition to cutting the sedimentary layers, it has a prismatic euhedral habit of regular size, transparent, vitreous luster and high crystallinity (Fig. 8J and K), possibly quartz crystals filled in the fractures (see Hartmann et al., 2012; Teixeira et al., 2018; De Vargas et al., 2022). The same crystallization rarely occurs in slides following the layering plane and covering the sedimentary structures and the dubiofossils (Fig. 8H and I), which makes it easier to distinguish the sticks from this filling.

365 The geological history of this outcrop is complex, resulting from a range of processes including synsedimentary/eodiagenetic processes, mesodiagenetic lithification, and thermal alteration during and after the intrusion of the sill. As a result, the origin of the dubiofossil may be linked to one or more of these processes, or their superimposition. Further investigation of similar products is therefore necessary to shed light on the potential origins of this dubiofossil.

3.2 Indigeneity and Syngenicity

370   Indigeneity and syngenicity are two concepts used to establish the origin and temporal history of materials. Indigeneity refers to the origin of the material and aims to eliminate the possibility of recent or procedural contamination. Syngenicity, on the other hand, seeks to establish synchronism between the material and its matrix or inserted medium, providing evidence of its temporal history (Buick, 1990; Wacey, 2009; McLoughlin and Grosch, 2015; Rouillard et al., 2021). In the case of the material under study, the brown cement coating over the dubiofossils and on the matrix suggests indigeneity, ruling out procedural

375   contamination (Fig. 5). Additionally, the presence of sticks predating the alteration and hematitic coat, which may have resulted from recent cementation (Al-Agha et al., 1995), supports this hypothesis. The cement is also found in parts of the filled fractures, and the crystallized layer covering the dubiofossils strongly suggests that the sticks are older than the fill and the intrusive rock (Fig. 8H-K). Therefore, the sticks likely predate or are synchronous with the placement of the intrusive rock. The dubiofossils always inserted in the clay or silt sheets indicate indigeneity, not growing later over the layers (Fig. 5 and 6).

380   The fact that the elongated minerals do not cut the laminations, cross, or disarrange the spheres may be an argument for a previous origin or during deposition/diagenesis (syngenicity). However, it does not rule out the possibility of a later growth taking advantage of the horizontal weakness of the sediment laminations and regions without spheres (e.g., Makovicky et al., 2006). Or it may indicate the concomitant metamorphic growth of spheres and sticks (Fig. 5). Therefore, the dubiofossil can be considered indigenous, but its syngenicity remains open.

385   ## 3.3 Comparison with similar objects

        The origin of the dubiofossils is suggested by the observed distribution of the sticks only close to the contact and prior to the filled veins linked to the intrusion. Formation by thermal effect is chemically plausible since ions and acids are produced by thermal degradation of organic matter (microbial C attested in the matrix) and by magma degassing capable of crystallizing these carbonates (Saxby and Stephenson, 1987; Aarnes et al., 2010; Agirrezabala et al., 2014; Liu et al., 2016). Nevertheless,

390   the morphology of the sticks is different from products of contact metamorphism in mudstones: 1) usually these carbonates are cements or pore fillers, occupying the available space and generally amorphous/subhedral and unbranched (e.g., Finkelman et al., 1998; Huntington et al., 2011); 2) they occur as fractures breaking the sedimentary layers, forming irregular, sharp to serrated branches; features missing from sticks (e.g., Golab et al., 2007; Huntington et al., 2011). As the origin by contact metamorphism seems implausible, the dubiofossils may be earlier and have been modified by the thermal effect resulting in

395   the calcitic composition found. In this way, the sticks were compared with several abiotic and biotic objects from similar contexts, regardless of composition, to assess the most likely origin. Controlled minerals from sponge spicules, skeletons of sea urchins and algae, minerals induced/influenced by fungi and bacteria, inorganic pre- and synsedimentary/eodiagenetic minerals such as evaporites, springs and other precipitations and mesodiagenetic crystals were surveyed looking for resemblances with the sticks, Fig. 10.

400
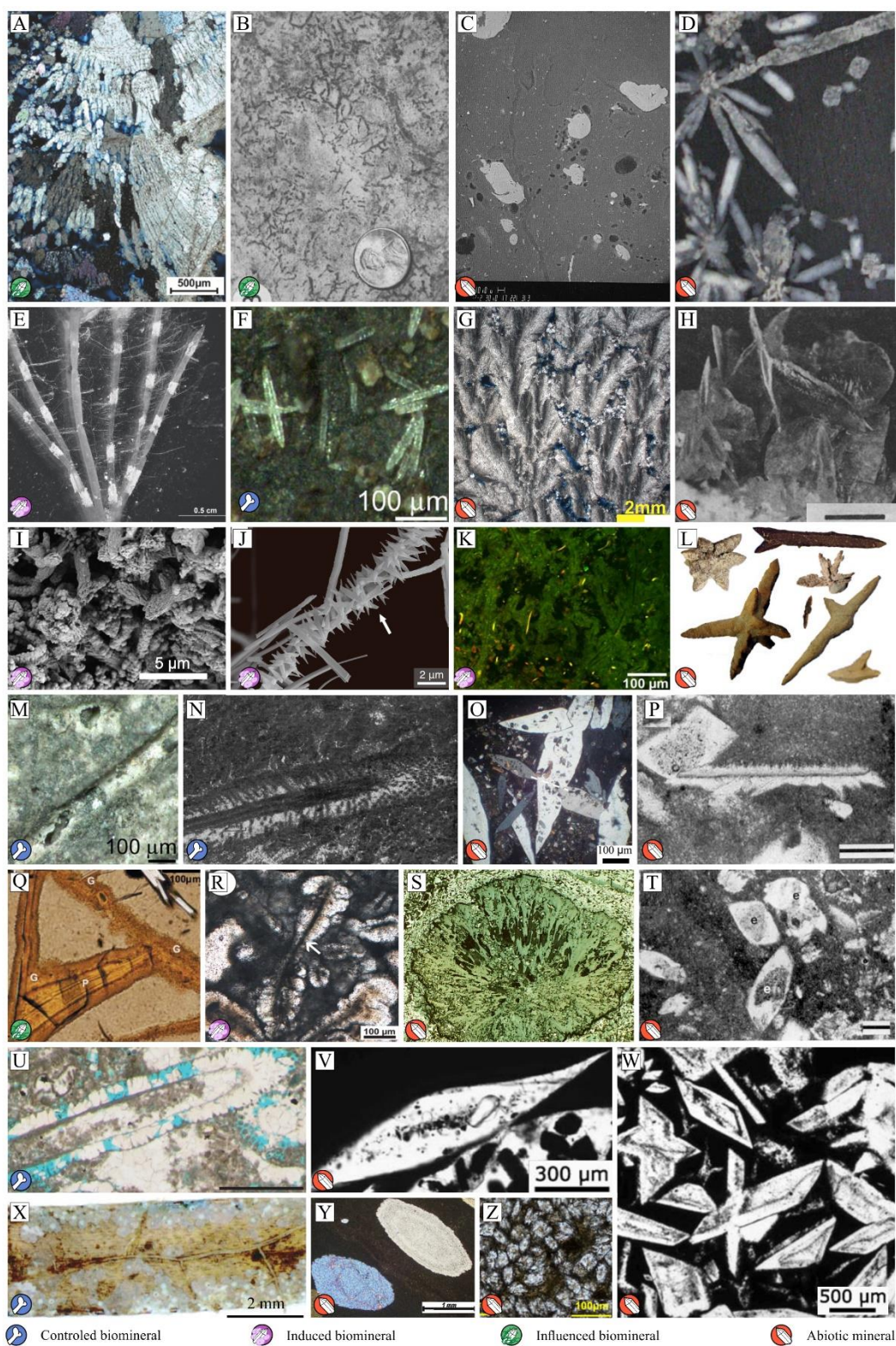
Figure 10: Comparison examples: A) Carbonate (CaCO3) influenced by bacteria, Kraus et al., (2018); **B)** Carbonatic rizolith (influenced substitution), Loope (1988); **C)** Calcite (light gray spheres) produced by thermometamophism in mudstone (dark gray), Finkelmann (1998); **D)** Chrysanthemum stone (diagenetic radial celestine - SrSO4); **E)** Carbonate precipitation over specific regions of the algae (induced crystallization), Apolinarska et al. (2011); **F)** Silicious sponge spicules (skeleton), Müller et al. (2006); **G)** Shrub-like arborescent evaporitic calcite, Farias et al. (2018); **H)** Evaporitic gypsum (CaSO4·2H2O), Garber et al. (1987); **I)** Tube like forms of induced calcite in microbail mat, Vasconcelos et al. (2006); **J)** Ramified and ornamented calcium oxalate produced by fungi (induced minerlization), Bindschedler et al. (2016); **K)** Vertical section of a modern microbial mat with a filamentous network inducing calcite crystallization, Arp et al. (2010); **L)** Diverse habits of glendonite (ikaite pseudomorph CaCO3·6H2O, cold water precipitation), Schultz et al. (2022); **M)** close view of sponge siliceous sponge spicule, internal detail (skeleton), Müller et al. (2006); **N)** Carbonate algae (skeleton), internal detail, Wolf, (1965); **O)** Thin section of evaporitic elongated gypsum (Aref & Mannaa, 2021); **P)** Diagenetic calcite (CaCO3), internal structures, Maliva (1989); **Q)** Vulcanic glass fractured containing banded palagonite (P) microbially deposited, (influenced), Mcloughlin et al., (2009); **R)** Tufa crystal with micritic central filament, with supposed biotic origin, (influenced), Della Porta (2015); **S)** Siderite (FeCO3) nodule from a thermal affected mudstone, Golab et al. (2007); **T)** Diagenetic calcite, internal details, Maliva (1989); **U)** Dasycladales (algae) in wackestone, original skeleton and mold, Granier (2012); **V)** Glauberine (CaNa2(SO4)2) evaporitic with inclusions of faecal pellets (influence not proved), Salvany et al. (2007); **W)** Zoned glauberine, evaporitic precipitation in substrate-water interface, Salvany et al. (2007); **X)** Coralline red algae growing on leaves of the seagrass (skeleton), Beavington-Penney et al. (2004); **Y)** Evaporitic sparse anhydrite (CaSO4) crystals in mudstones, concentrically zoned, Aleali et al. (2013); **Z)** Diagenetic siderite presenting internal impurities, Wang et al. (2021).

Most objects observed had similarities to the elements of dubiofossils described in Sect. 3.1, including their external form, internal structures, texture, and composition. The random distribution, packing and branching seen in the objects is similar to that of algae and fungi, as well as evaporitic, tufaceous, and diagenetic minerals. The internal features, such as variations in

405 crystallinity and a dark central axis, may resemble internal structures of algal skeletons and sponge spicules or features of induction/influence of algae, bacteria, or fungi, nevertheless they may also be diagnostic textures produced by diagenetic processes.

The wide range of morphologies observed among the sticks made it difficult to immediately associate them with any of the compared products. Each morphotype or shape class could be associated with a specific object, but when compared to another

410 class, the association appeared less likely. For example, radial forms of class C with tapered ends (Fig. 4E and F) strongly resemble "Chrysanthemum Stones" (eodiagenetic mineralization of celestine or calcite; see Makovicky et al., 2006; Fig. 10D), while comparing with the other classes they are very distinct. However, the morphological complexity does not necessarily indicate a higher probability of biogenic origins (McLoughlin and Grosch, 2015), since, complex and diverse forms are common in depositional minerals such as calcite and gypsum (see Maiklem et al., 1969; Garber et al., 1987; Aleali et al., 2013;

415 Schultz et al. 2022; Fig. 10H), as well as diagenetic minerals (e.g., diagenetic calcites; Maliva, 1989; Ren and Jones, 2021; Fig. 10P, and T).

The internal organization in layers, textural and compositional variations found in the sticks do not refer to specific mineral products. However, the features described here resemble layered structures, central features and other textures produced by bacteria and fungi, which during their formation and growth generate zoned minerals and cell, hyphae or EPS allocation site

420 within the biomineral (e.g., Golubic et al., 2000; Arp et al., 2010; Dellaporta, 2015; Bindschedler et al, 2016). On the other hand, these features also resemble zonations, inclusions, and areas of impurities generated during diagenetic mineral growth (e.g., Maliva, 1989).

Comparing the matrix relationships of dubiofossils and other products can be problematic due to morphological variability. Flat, 2D topologies and impressions that accompany lamination may resemble diagenetic minerals (e.g., Maliva, 1989; Makovicky et al., 2006), while 3D features such as tubular or flattened shapes that do not cut through layers may resemble pre- and syndepositional objects, such as evaporitic, tufaceous, and biominerals (e.g., Babel, 2004, Vasconcelos et al., 2006). Additionally, mineralized structures that do not cut through layers can also occur as a result of diagenetic growth (e.g., Makovicky et al., 2006).

The comparison revealed a low likelihood that the dubiofossil is a controlled biomineral. Skeletal biominerals typically exhibit greater regularity in size, shape, and branching due to their specific physiological origins (Dupraz et al., 2009). For instance, despite similarities to sponge diactinal spicules (such as tapered ends, outer layers, and dark central feature thought to be axial filament, as seen in Uriz et al., 2003; Weaver and Morse, 2003; Müller et al., 2006; Fig. 10F and M), the dubiofossil's irregular branches in angle (ranging from 8º to 90º with the main axis) and length, as well as the morphological variations between classes, make this hypothesis less likely. Therefore, the absence of a controlled angular pattern or branching spacing and the wide variation in shapes precludes classification as a skeletal biomineral from sources such as sponge, sea urchin, coral, and coralline algae (Fig. 10A, N, U and X; e.g., Wolf, 1965; Hooper and Van Soest, 2002; Beavington-Penney et al., 2004; Sethmann and Whörheide, 2008; Leonov et al., 2009; Granier, 2012; Grgasović, 2022).

Regarding the composition, minerals (abiotic and biotic) with similar composition and capable to posterior calcitic replacement were surveyed: carbonates and calcium sulphates. Some of these minerals were excluded from the comparison because they did not have an origin compatible with the context observed for the sticks, such as aragonite, magnesite, gaylussite, ankerite, and kutnohorite (Lippmann, 1973; Alhaddad and Ahmed, 2022; Xu et al., 2019; Reijmer, 2021). The rest can be deposited abiotically as evaporites, biotically by bacteria or by diagenetic crystallization. Most may have elongated habits like sticks, but only calcite, ikaite, gaylussite, gypsum and dolomite commonly have the diversity of habits of dubiofóssil: radial, laterally branched and elongated. Even, specific stick's patterns of size, shape and distribution have not been found in the literature for these minerals (e.g., Warren, 2000, 2010; Babel, 2004; Schultz et al., 2022). Therefore, the shape may be the result of further thermal modification of the material and therefore vaterite, siderite, dawsonite, gypsum/anhydrite also remain as putative original materials. As the comparison did not result in a more likely hypothesis, the proposals will be further evaluated in the next section.

3.4 Evaluating proposals

How to proceed when comparison with objects from the literature does not significantly reduce the number of possibilities for the dubiofossil? Although controlled biomineral hypotheses have been eliminated, the descriptive and visual comparison of the dubiofossil did not yield a conclusive result. Therefore, a detailed discussion is necessary to determine its proposed origin. The lack of comparative parallels suggests that the complex environmental conditions in which it was formed – a transitional environment with strong climatic influences, such as variations in temperature, water volume, salinity, and mixing of saline and continental waters, in addition to a significant interface with extensive microbial mats – played a crucial role in shaping

the final composition and morphology of the material. The dubiofossil underwent common diagenesis during the Itararé strata formation and subsequently experienced thermal effects resulting from the Cretaceous intrusion. Accordingly, dubiofossils seem to be the result of this complex history due to: 1) the large population morphology range that prevents the identification of the material as a product that is only depositional or diagenetic or metamorphic or biotic mediated by microbial mats; 2) a

460   distribution restricted to this contact that does not occur far from it in the previous layers of the Rio do Sul Formation, which disfavors the explanation of a purely depositional product, whether abiotic or biotic; 3) a relatively wide geographic distribution, occurring in the three outcrops always closer to the sill contact but not found in other Cretaceous thermal aureoles within the Paraná Basin (see Santos et al., 2009; Hartmann et al., 2012; Teixeira et al., 2018; De Vargas et al., 2022), which precludes characterization as an artifact of purely contact metamorphism. Thus, the dubiofossil may have been formed through

465   the combination of a syndepositional or diagenetic process with thermal effect.

3.4.1 Syndepositional or diagenetic product

Based on the hypothesis of a subsequent thermal alteration that modified and replaced the sticks, the original conditions of the material are evaluated, whether syndepositional or diagenetic, induced/influenced biominerals or abiotic minerals. To test the sticks as a pre-thermal mineral, the minerals selected in Sect. 3.3 are evaluated.

470   Gypsum – evaporitic mineral: The interpretation of sticks as evaporitic gypsum (and anhydrite as gypsum that loss water) is supported by shape and context. Elongated and radiated morphologies are common for non-agglomerated crystals, as well as tapered points (Babel 2004; Warren, 2016). Furthermore, the size fits the definition of selenite (gypsum >2 mm in length) which evidences subaqueous evaporitic deposition (Babel, 2004). In this way, the proximity to the sea could contribute with the necessary salinity, the semi-arid to arid conditions would favor evaporation and climate control such as cycles of melting

475   and freshwater input would generate temperature changes, brine mixing or brine freezing/freeze drying that together would culminate in the crystallization of the sticks (Babel, 2004; Warren, 2010). The low or no salinity inferred by the trace fossils (see Netto et al., 2009), does not interfere with the presence of these evaporites, only saturation in calcium sulfate is required, in addition, more saline moments and intense stratification could be seasonally or daily controlled in a monomictic to polymictic lake (see Babel, 2004; Ayllón-Quevedo et al., 2007). The presence of sticks in the top section of the quarry is

480   indicative of these specific conditions of higher salinity inferred by the reduction of trace fossils, contrary to the base of the quarry with more trace fossils and shallower conditions, more conducive to dissolution by the input and interference of fresh water (Babel, 2004). Microbial mats, common in evaporitic systems (Trichet et al., 2001; Bontognali et al., 2010; Warren, 2010, 2016; Perillo et al., 2019), would favor the preservation of the sticks on and within mats, as the gas domes indicate low substrate permeability, allowing the concentration of ions for precipitation (e.g., Paso Seco, in Argentina, Perillo et al., 2019).

485   Thus, evaporitic gypsum precipitation is plausible in this context, requiring by the Usiglio precipitation sequence, the deposition of carbonates before sulfates (see Babel, 2004; Warren, 2010). In addition, these earlier carbonates may have replaced the gypsum sticks by the Cretaceous thermal effect.

Ikaite – depositional/eodiagenetic mineral: composition, multiple external branching forms and internal features may denote origin as ikaite. Although the specific conditions of formation of this mineral are still little known, they occur as surface
490 precipitated minerals (e.g., Oehlerich et al., 2013) or eodiagenetic (Lu et al., 2012; Zhou et al., 2015) in multiples cold water environments (continental to abyssal; see Rogov et al., 2022 and Schultz et al., 2022 for a review). These crystals are extremely unstable, quickly dissolving or changing to glendonite (a variety of calcite that replaces ikaite, Huggett et al., 2005; Schultz et al., 2022). The multiple shapes of the sticks match the morphologies of this unstable mineral (Schultz et al., 2022). The central internal features rich in iron and magnesium (e.g., Schubert et al., 1997) may be nuclei of magnesium ions that would guarantee
495 mineral stability (Purgstaller et al., 2017; Stockmann et al., 2018) and the concentric layers may be marks of the transformation of ikaite into glendonite (proposed by Vickers et al., 2018). This mineralization can occur in the sulfate reduction zone or in the sulfate-methane transition, well established by microbial mats, whose high pH and organic content also favor the maintenance of ikaite, promote the glendonite replacement and prevent the dissolution (see Lu et al., 2012; Zhou et al., 2015; Trampe et al., 2016). The mat can also contribute to rise the phosphorous content related to the ikaite stability, like hyper-
500 eutrophy in Manito Lake – Canada (Last et al., 2013), once calcium phosphate was reported by Callefo et al. (2019b) in similar Itararé outcrop linked to MISS. Furthermore, the occurrence of sticks on some of the top laminae of the outcrop section could be caused by climate or environmental control, such colder seasonal moments of the lake, or specific depth conditions (see Oehlerich et al., 2013 and Schultz et al., 2022).

Dolomite – syndepositional or eodiagenetic precipitation: the context interpreted for the sticks fits into some of the various
505 subenvironments and conditions in which dolomite can form and together with the texture of the dubiofossils, make this interpretation plausible. Cloudy centered and clear-rimmed crystals are common textures in dolomites, denoting the replacement of high Mg-calcite by dolomite and the increase in order and size during diagenesis, since these minerals tend to age/evolve throughout burial history (Sibley et al., 1994; Warren, 2000; Ayllón-Quevedo et al., 2007). As syndepositional dolomites in evaporitic environments (similar to gypsum discussed above), marine and lacustrine tend to form laminae or
510 surface strata (Warren, 2000; Trichet et al., 2001; Babel 2004), the pattern of distribution and packing of sticks has greater resemblance to eodiagenetic products such as interstitial, intrapore or intramat mineralization (Warren, 2000). The eodiagenetic sticks can be mixing zone dolomite or hemipelagic organogenic products (see Warren, 2000). The transitional conditions interpreted for the outcrop allow the mixing of a phreatic pore water close to saturation in calcite with a fresh water that leads to a state of undersaturation (Warren, 2000), with the mineral growing as void-fillings in the mixing zone (Ward and
515 Halley, 1985). The other plausible explanation is the origin of the sticks related to the subsurface degradation of layers rich in organic matter and the increase in alkalinity in the zones of sulfate reduction or methanogenesis, well developed at the outcrop and diagnosed by the gas domes of the mats, which would favor mineralization (Roberts et al., 2004; Wright and Wacey, 2004; 2005). Several authors point to the reduction of sulfate by bacteria as essential and link most occurrences of eodiagenetic dolomite to the presence and mediation of microbial mats (Roberts et al., 2004; Wright and Wacey, 2004; Vasconcelos et al.,
520 2006; Bontognali et. al., 2010). Thus, the interaction of the MISS with the sticks reinforces this hypothesis, since the mats are preponderant for crystallization, acting as nucleation centers (Vasconcelos et al., 1995).

Calcite – abiotic mineral: The sticks can be made of calcite, as it fits into the various subenvironments, depositional and diagenetic contexts presented in the previous hypotheses as marginal evaporites, diagenetic products, or the result of biotic interaction with the environment and can generate unconventional and/or multiples forms of calcites (e.g., Wright and Barnett, 2015; Payandi-Rolland et al., 2019). In chemical and evaporitic deposits, shrub-like, dendritic, stellate, and spheroidal forms are abiotically precipitated (Wright and Barnett, 2015; Kraus et al., 2018; Farias et al., 2019), controlled or modified by the presence of Mg^{2+}, which can, for example, promote growth parallel to the crystalline c-axis (Zhu et al., 2006). Thus, the presence of this element in the water, in the conditions of a restricted or saline lake, can be the justification for the unusual precipitation of the sticks, maintaining the centers rich in magnesium. Most diagenetic calcites are amorphous and fill the pores of the sediment like cement, originating from the concentration of Ca^{2+} in the interstitial space, however there are occurrences of euhedral and distinct forms, with the presence of relicts and growth in layers (Cardoso, Basilici and Silva, 2022; Sommer, Kuchle and De Ros, 2022), thus the sticks may have formed during diagenesis, with the dark center as a relict and impurities that favored its growth and the final shape modified by metamorphism.

Calcite – bimineral: many authors emphasize the importance of sulphate bacteria, cyanobacteria, microbial mats and EPS in syndepositional and eodiagenetic calcite crystallization (Kropp et al., 1996; 1997; Bosak and Newmann, 2005; Baumgartner et al., 2006; Vasconcelos et al., 2006; Dupraz et al., 2009; Arp et al., 2010, among others). In this sense, the formation of sticks may be related to the organic content of the mats in three degrees of relevance. The first results from the presence of the mat with EPS only as a nucleation center, providing carboxyl groups for the initial binding of Ca^{2+} ions from water and subsequent abiotic growth of calcite (Turner and Jones, 2005; Baumgartner et al., 2006). In the second degree, in addition to serving as a nucleus, the degradation of bacteria and EPS (CO_2- degassing) may have influenced mineral growth by establishing a favorable microenvironment (pH, [Ca^{2+}], alkalinity, temperature), moreover, the distribution of EPS on the mat can serve as a crystallization template, which partially explains the arrangement of sticks in the matrix (Kropp et al., 1996; 1997; Turner and Jones, 2005; Spadaforda et al., 2010; Arp et al., 2010; Payandi-Rolland et al., 2019). In the third degree, in addition to serving as a nucleation center, the metabolism of bacteria, whether sulfate reducers or cyanobacteria, may have induced the crystallization of the sticks (Kropp et al., 1997; Bosak and Newmann, 2005; Baumgatner et al., 2006; Vasconcelos et al., 2006; Spadaforda et al., 2010). Kropp et al. (1997) exemplified this EPS control on carbonates in temperate water intertidal siliciclastic sediments. Microorganisms can control calcification by secreting inhibitors and influencing binding of Ca^{2+} and Mg^{2+} ions (Braissant et al., 2003; Bosak and Newmann, 2005; Arp et al., 2010). The bacterial metabolism and EPS degradation promotes the precipitation of ovoids carbonates, the continued degradation favors the aggregation and formation of larger ovoid crystals (e.g., Spadaforda et al., 2010; Payandi-Rolland et al., 2019). The variety of stick morphologies, also recognized in induced/influenced biominerals of current biofilms, can be explained by the transformation from one form to another over time, changes in EPS chemistry during crystallization or modifications in the degree of supersaturation of carbonates (Turner and Jones, 2005; Spadaforda et al., 2010; Arp et al., 2010; Liang et al., 2013; Payandi-Rolland et al., 2019). In addition, the shape may be an exotic deviation produced by unique physicochemical conditions such as the calcite dendrites reported by Turner and Jones (2005), which would have undergone further thermal modification.

Other carbonate minerals: the sticks can be other carbonate minerals, in which have less diversity of habits and morphologies, and generally presented in relatively smaller spheres than the sticks, despite that, de final form of the sticks can be caused by metamorphism. Although vaterite is a very rare mineral vaterite, found mainly as a controlled biomineral of mollusk shells, the sticks can be a rare depositional occurrence associated with bacteria usually forming microspheres (is required high NH3

560 and high pH, to promote the carbonate supersaturation, easily achieved in the mat), once naturally precipitated it has low stability and tendency to recrystallization the morphology is easily modified (Lippmann, 1973; Rodriguez-Navarro et al., 2007). Dawsonite is a common authigenic mineral that can have an acicular shape, more elongated than stick of classes A and B, usually it forms in the eodiagenesis of continental alkaline saline environments, when pore water is concentrated in Al, or in mesodiagenetic CO2 storage environments (Eugster, 1980; Hellevang et al., 2013; Xia et al., 2022), however, Al was

565 detected inside and out of the dubiofossils. The sticks can be siderite growing during eodiagenesis as cement in pore water by the decomposition of organic matter, with methanogenesis produced in highly reducing anoxic non-sulphidic environments, whether lake, lagoon or marine (Mücke, 2006; Vuillemin et al., 2019; Lin et al., 2020), that fits the Bemara interpretation. Several authors emphasize the mediation of sulfate-reducing bacteria in the process and others point to the presence of Mg that helps in the reaction (Sapota, et al., 2006; Lin et al., 2019).

570 Evaluating the proposals within the complex context of the sticks and considering the analyzed composition as probably a thermal modification. It is possible, based on the descriptive criteria (Sect. 3.1) to relate the sticks' chances of being each of these proposed minerals. Although plausible, gypsum needs prior precipitation of carbonates (Babel, 2004), which leads to the question: how did the carbonate precipitate to favor the growth of these sticks? For dawsonite, it is not proved the alkalinity conditions. For vaterite is required specific conditions of high pH, NH3 and supersaturation (see Rodrigues-Navarro et al.,

575 2007), also not proved, but more possible because of the presence of bacteria. The other proposals remain with equal weight, as all of them show multiple forms, with similar textures and internal features. The compositional details and the distribution of elements contribute to keep the proposals valid, the presence of Mg and Fe mainly inside the structures can be the centers of nucleation of the material. For ikaite and siderite, magnesium may have favored its stability (Purgstaller et al., 2017; Lin et al., 2019), for calcite it could contribute to the generation of unusual external forms (see Zhu et al., 2006) and for dolomite, it

580 may be the trace of the original ions that, when replaced by Ca in metamorphism, were separated into the inside. Fe can still be a strong indication of the existence of organic matter, as a filamentous structure or EPS, which, due to the following mesodiagenetic, metamorphic and epigenetic reactions, was replaced/complexed by this element (see Roden et al., 2010; Kunoh et al., 2016; Lepot et al., 2017), favoring more the hypotheses linked to microbial mats.

3.4.2 Thermal effect

585 The effect of the intrusion on the sedimentary package is evidenced by the greater hardness in contact and the presence of multiple fractures and veins, in addition to the thermal effect indirectly diagnosed by altered palymorphs (Silva, 2020) in an aureole with gradual reduction of thermoalteration up to 2.5 m below the contact, which agrees with the model proposed by Aarnes et al. (2010) of aureole thickness of up to 200% of the thickness of their respective sills, in this case ~50% (see Silva,

2020). Two more features may be evidence of this metamorphism: 1) the matrix spheres described as clays may be metamorphic mineral such chlorite, which explains the interior impurity features and rounded to straight outer walls as a result of thermal growth (see Brammall, 1915; Weaver, 1984; Pitra and Waal, 2001). As the spheres are never cut by the sticks, it is possible that there was a later or concomitant development; 2) the sticks themselves with impurity and zoning features and final calcite composition may be due to metamorphism.

Several authors highlight the presence of carbonates in shales and coals only close to the contact of sills and dikes, generated by the thermal alteration of organic matter (Saxby and Stephanson, 1987; Meyers and Simoneit, 1999; Santos et al., 2009; Agirrezabala et al., 2014; Liu et al., 2016 and references therein). This reaction, by mineral dehydration and organic matter decarbonization/decomposition, produces inorganic and organic acids such as CO, CO_2, CH_4, HCO_3^- and water, besides the intrusion adds alkali cation (Fe^{2+}, Mg^{2+}, and Ca^{2+}), which together can circulate the sedimentary package by hydrothermal convection (Finkelman et al., 1998; Agirrezabala et al., 2014; Liu et al., 2016). This highly acidic environment can cause the dissolution of pre-existing carbonates and the precipitation of new ones (generally cementing the pores) by decreasing hydrothermal flow, overpressure buildup and ion concentration (Zekri et al., 2009; Liu et al., 2016). The conditions presented above support the presence of sticks only in this thermal aureole, but do not justify their morphological diversity, pattern of distribution between layers and packing.

Compositional differences in carbonates have been found to be linked to their proximity to intrusive bodies, with varying percentages of calcite, ankerite, dolomite, and siderite observed along the aureole, resulting from differences in Fe and Mg contents (Kisch and Taylor, 1966). These variations are influenced by the chemistry of the intrusive body, its distance from the dike or sill, and diagenesis specific to each thermal event (Finkelman et al., 1998). Furthermore, the petrophysical and chemical properties of the sedimentary package can also affect the circulation of fluids and the precipitation of carbonates, with mudstones contributing to overpressure buildup due to their very low permeability (Brace, 1980; Gerdes and Baumgartner, 1998; Aarnes et al., 2012; Agirrezabala et al., 2014). As a result, the variation in the sticks can be partially explained by the heterogeneity and differences in saturation, diffusion, and viscosity between mudstones and siltstones, as well as their distance from the contact (see Brace, 1980; Douglas and Beveridge, 1998; Mason et al., 2010; Sánchez-Navas et al., 2012).

3.5 Deciphering the complex history

615 Based on the proposed physicochemical conditions, it is possible to partially reconstruct the complex history of the sticks. This history resulted from overlapping processes and the evolution of depositional, eodiagenetic, mesodiagenetic, and metamorphic environments. The following discussion aims to link the various features of the sticks to these stages of the geological cycle, Fig. 11.
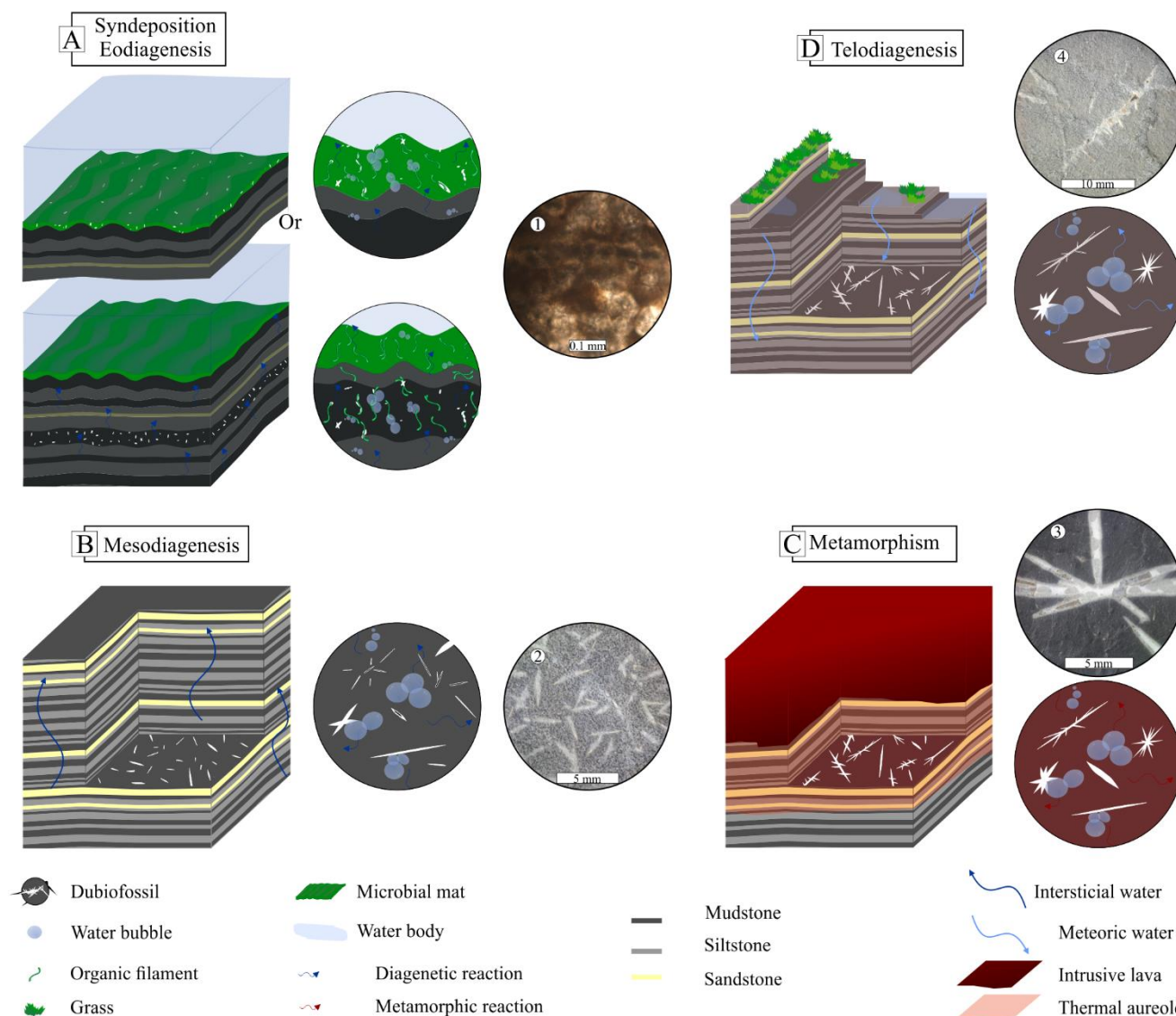
Figure 11: History of the formation of dubiofossils. A) Syndepositional or eodiagenesis associated with microbial mats, upper model deposition on the mat in life, lower, authigenesis in eodiagenesis by mat degradation; B) Mesodiagenesis and mineralization modifications; C) thermal effect, dissolution, modification, and replacement of the initial minerals by calcite and precipitation; D) telodiagenesis process of oxidation and cementation by hematite in recent exposure. 1-4) examples of the result of interpreted processes.

The carbonates discussed above, including ikaite, dolomite, calcite, and siderite, are more likely associated with microbial

620   mats, whether syndepositional or diagenetic (Fig. 11A). The occurrence of sticks with mats suggests an unlikely abiotic origin. The distribution of crystals may have been morphologically controlled by the EPS or the bacteria, serving as nucleation centers (Arp et al., 2010; Payandi-Rolland et al., 2019). However, it is unlikely that the EPS withstood later diagenetic and thermal modifications (see Turner and Jones, 2005), resulting in the transformation of the dark central axes to iron and magnesium. The rare occurrence of a dark central axis lining mineralized circles may indicate the original mineralization (see No. 1 in Fig.

625   11).

The form of sticks may be linked to branched mineral habits, which are common in ikaite and less frequent in dolomite and calcite, as well as to the mineral evolution over time due to deposition and diagenesis processes that tend to modify or age them (see Warren, 2000; Payandi-Rolland et al., 2019; Schultz et al., 2022). Growth may have occurred abiotically after nucleation, driven by the physicochemical conditions of the microenvironment (see Turner and Jones, 2005), which are specific

630   to each mineral, as discussed in Sect. 3.4. Alternatively, the metabolism or degradation of the microbial mat may have induced or influenced the transformation of these crystals, causing the ovoids to unite into elongated structures and resulting in elongated or branched crystals with central axes (see Spadaforda et al., 2010).

The evolution of these minerals may have been mediated by the eodiagenetic alteration of the mat, as evidenced by the gas domes, the degradation of the organic content, which established methanogenetic or sulfate-reducing conditions and

635   contributed to morphological transformations. Changes in the chemistry of EPS or modifications in the degree of carbonate supersaturation may also have played a role (Fig. 11A; Warren, 2000; Wright and Wacey, 2004; Turner and Jones, 2005; Zhou et al., 2015; Payandi-Rolland et al., 2019).

Crystallization commonly occurs around filaments or EPS in laboratory and modern environments, where it tends to grow vertically alongside biofilms (Pratt et al., 2001; Vasconcelos et al., 2006; Arp et al., 2010). However, in some cases, purely

640   horizontal occurrences may be the result of water loss from clays and subsequent diagenetic flattening. Other modifications may have taken place during diagenesis, such as the complete replacement of ikaite by glendonite, or crystallographic changes in dolomite and calcite (Fig. 11B).

Contact metamorphism is believed to be the primary modifying agent responsible for the observed phenomena (Fig. 11C). The thermal effect of the intrusion likely contributed to the simultaneous growth of matrix spheres and sticks. This thermal

645   alteration may have also caused the acidification and significant degradation of organic matter, which could have dissolved previous carbonate minerals and recrystallized and precipitated calcite (as described by Liu et al., 2016), replacing the original calcite, dolomite, siderite, or ikaite/glendonite. As a result of this process, impurity separation features may have formed, creating a dark center and Ca-rich external layers, which may or may not retain the central axis structure. Additionally, recrystallization and precipitation may have facilitated the union of aligned smaller sticks to form larger sticks, with branches

650   composed of other mineralized tubes that were fused to the axis, resulting in the morphologies of class B, (see No. 4 in Fig. 11). The irregularity in branching angles can be attributed to the random distribution of EPS or filaments that served as nuclei

within the matrix. Thermal alteration-induced precipitation may have generated radial morphologies of class C and D (see No. in Fig. 11), starting from a core, such as an old EPS/cell or a pre-existing mineralized structure.

The observed variations in morphologies between classes A, B, C, and D linked to the color of the matrix, appear to be related
to initial sedimentological differences (variations in the amounts of mud and silt between layers), the amount of organic matter and original crystals, and specific physicochemical conditions during thermometamorphism and contact distance (Brace, 1980; Finkelman et al., 1998). For example, Class C, occurring in darker mud layers, seems to have lower permeability, resulting in larger radial shapes (see No. 3 in Fig. 11). Conversely, the smaller sticks of Class A, linked to the light gray matrix, appear to be less influenced by reprecipitation and possibly retain an appearance closer to the original with a central "filament" and
without the growth of long sticks, possibly due to greater relative permeability or lesser amounts of organic matter to be degraded at that level (see No. 2 in Fig. 11). Class B may have sufficient organic matter and permeability to reprecipitate, grow, and unify the crystals into elongated branched forms. Class C appears to have higher permeability, keeping the crystals as separate rods, with less permeable regions or organic cores allowing for the growth of radial dots.

During the final intrusion process, both vertical and horizontal fractures were filled with quartz, likely as a result of
hydrothermalism, as observed in other sedimentary sections of the Paraná Basin with the intrusive suite of the Paraná-Entendeka LIP (e.g., Hartmann et al., 2012; Teixeira et al., 2018). Finally, the recent exposure of the outcrop resulted in hematite oxidation, cementation in the matrix spaces, covering the spheres and sticks and replacing the organic "filaments" inside the sticks (Fig. 11D).

3.5.1 Remaining questions

Does the composition found indicate that the original composition was not calcite? Despite, according to the data, calcite is the main material present, the distribution of elements found by EDS suggests that regions of high calcium concentration are mainly found around the sticks, with iron and magnesium located in the center and the matrix. This raises questions about whether Fe and Mg should have covered a smaller area if they were only impurities in the original calcite. One possibility is that the concentration of these elements indicates the presence of another mineral, either original or substituted during
metamorphism, such as ankerite, siderite, dolomite or high Mg-calcite.

If these morphologies are mineralized by microbial mats, why are features with a certain similarity not found at the base of the outcrop? For this, three possible explanations are suggested. One is that environmental factors, such as depth or circulation, may have restricted deposition to only the top of the Bemara section. Another possibility is that some diagenetic or recent process consumed the mineral from the sticks far from the thermal aureole, as metamorphism may have conditioned greater
resistance to weathering. The third option is that mineralization was entirely promoted by the thermal effect, with the intrusion contributing ions and degrading the organic matter necessary for calcite crystallization. The sticks may have used the filamentous structure of fossilized EPS as a template for growth in different forms, which would justify their absence away from contact.

Although the hypothesis discussed above considers the possibility of biofilms and the sticks being involved in the
685   mineralization process, it is still unclear whether the abiotic hypotheses is completely refuted. Two hypotheses can be tested:
one is that the sticks are depositional/diagenetic abiotic calcite, which, due to specific geochemical conditions (such as the
influence of Mg2+ ions on growth; see Zhu et al., 2006), could result in the exotic forms found. The second is that the rods are
purely metamorphic abiotic calcite, since internal features of opaque axis in the center, compositional changes, crystallinity,
and zonation can also be produced by metamorphism (Pitra and Waal, 2001; Mason and Liu, 2018). With the varied shapes
690   and distribution being explained by physicochemical conditions of the substrate and intrusion (Brace, 1980; Finkelman et al.,
1998; Agirrezabala et al., 2014).

Considering the current proposal of the ubiquity of life across the Earth's crust (see Merino et al., 2019; MacMahon and
Ivarsson 2019), is it possible that both early mineralization (sydepositional or diagenetic) and thermal modification are
mediated by bacteria? Although few studies have been conducted on this topic (Bengtson et al., 2017; Ivarsson et al., 2020,
695   2021), the heat of the intrusion, the presence of organic material, and the chemical reactions involved could create favorable
conditions for the establishment of a deep biosphere that would help increase the diversity and complexity of stick
morphologies. However, the lack of information prevents testing this hypothesis, so it is unclear whether the occurrence is
mostly biotic.

3.5 Biogenicity criteria for bio- and biomimetic minerals

700   The sticks described in this study demonstrate the lack of conclusive evidence for the biogenicity of biominerals and inorganic
minerals. Despite a thorough description and comparison, there were not enough convincing arguments to discard any
hypothesis, although an origin as a controlled biomineral seems less likely. The size, shape, structure, texture, and arrangement
with the matrix observed in the sticks are not necessarily diagnostic of abiotic or biotic products. These characteristics can be
present in natural materials regardless of their origin, which is consistent with the views of several authors who have
705   emphasized the challenges of using these features as biogenicity criteria (García-Ruiz et al., 2002; Weiner and Dove, 2003;
McLoughlin and Grosch, 2015; McMahon et al., 2021; Rouillard et al., 2021; McMahon and Cosmidis, 2022). This highlights
the importance of further investigation of both biominerals and biomimetic inorganic minerals (Dupraz et al., 2009).

The irregular spacing and periodicity of branches observed in the sticks are not typical of controlled biominerals, but rather
common in induced, influenced, and abiotic biominerals (e.g., Shearman et al., 1989; Bindschedler et al., 2014). The
710   composition of calcite, a mineral produced by various abiotic and biotic processes (Maliva, 1989; Weiner and Dove, 2003;
Davies and Smith, 2006; Babel, 2007; Salvany et al., 2007; Benzerara and Menguy, 2009; Warren, 2016; Benzerara, Bernard
and Miot, 2019), is a result of complex histories and thermal transformations, making it challenging to eliminate any
hypothesis. Furthermore, the biotic origin of the sticks is supported by their co-occurrence with microbial mats, a feature that
is associated in the literature with the crystallization of several minerals, whether induced or influenced. However, in
715   transitional environments, abiotic crystallizations are also common (see Warren, 2000; Babel, 2004; Noffke, 2010).

The high variability in morphology and taphonomic characteristics has often been used as evidence of biogenicity for microfossil-like and biomineral-like objects (Whitney, 1989; Buick, 1990; Verrecchia and Verrecchia, 1994; Douglas and Beveridge, 1998; Wiener and Dove, 2003; Dodd et al., 2017). However, as demonstrated by the sticks, this variability can also be the result of a complex history involving overlapping processes, physicochemical and microenvironmental variations, and
720 other factors, making it a less conclusive criterion for mineral biogenicity.

Although the descriptive survey and comparison provide strong evidence for a biogenic origin of the sticks, it is still not possible to completely rule out an abiotic hypothesis. Therefore, the sticks exemplify the challenges of investigating biominerals and highlight the need to consider the complex history, superimposed processes, and ubiquity of life in the investigation of biomineral-like objects.

725 **4 Conclusion**

We have proposed a descriptive protocol for dubiofossils, building upon previous work. Our protocol comprises four classes of attributes: morphology, structure, and texture; relationship with the matrix; composition; and context. By examining these attributes, we can infer details that help us determine whether dubiofossils are indigenous and syngenetic and compare them to similar biotic and abiotic objects. Itararé's dubiofossils are products of nature, and their wide range of morphologies makes
730 them distinct from any known minerals. The complexity of their geological history and the various processes that contributed to their formation are responsible for this difference. Therefore, we suggest that dubiofossils are likely the result of a combination of processes and a complex geological history.

1)   Environment: The establishment of a transitional setting, characterized by a shallow lake close to the sea and the reception of continental deglaciation fluxes, in conjunction with semiarid conditions that are capable of reducing the water
735 column and extensive microbial mat at the bottom. This environment provides many possibilities for the presence of original minerals, such as evaporitic gypsum, depositional/eodiagenetic ikaite and dolomite, abiotic calcite, biofilm-mediated calcite, and eodiagenetic vaterite, dawsonite, or siderite. Although the co-occurrence with MISS reinforces the likelihood of biotic origin, the possibility of an abiotic origin cannot be completely ruled out.

2)   First precipitation: regardless of the type of mineral, the deposition occurred on or within the mats (underwater or
740 eodiagenetic conditions) in which the EPS and bacterial filamentous structures would serve as nucleation centers. In which initial spheres would deposit by influence or induction of bacteria.

3)   Diagenesis: the various eo- and mesodiagenetic chemical reactions, including mat degradation, would serve to modify and aging the crystals, aggregating spheres in rods or growing ramifications.

4)   Intrusion and thermal alteration: the intrusion of a sill from the Serra Geral Group has caused significant changes in
745 the sedimentary package in contact. The heat generated by the intrusion led to the occurrence of new reactions, high degradation of organic matter, dissolution, reprecipitation, and replacement of original minerals by calcite. These

thermometamorphic processes have resulted in a considerable variability in forms, primarily due to physicochemical differences in the matrix.

5)   Posterior processes: quartz filling of fractures and veins at the end of intrusion (Cretaceous) and cementation/hematite replacement in the matrix by telodiagenetic exposure (recent).

The sticks described in this study serve as an example of how complex morphologies, wide range morphology, organized textures, and composition can be the result of a complex history for dubiofossils. Therefore, these attributes should be carefully investigated and used with caution as evidence of biogenicity for biomineral-like objects. It is important to note that exotic forms can be present in both abiotic and biotic products of nature, emphasizing the need for thorough analysis and evaluation.

Data availability: data presented in this work can be shared upon request.

Author contribution: JPS designed the study with help from JC and RSH. JPS conducted the study with technical assistance from MLAFP and LDM. All co-authors analyzed the results. JPS prepared the manuscript with contributions from all co-authors.

Competing interests: The authors declare that they have no conflict of interest.

Acknowledgements: We appreciate and are thankful for the support of the Universidade do Vale do Rio do Sinos, Universidade Federal de Santa Catarina, and ITT OCEANEON. We are grateful for the advice and discussions with Professor Joseph Botting, Professor Francisco Manoel Wohnrath Tognoli, Professor Cristina Silveira Vega, Professor Heinrich Frank and Professor Andrea Sander, especially Professor Renata Guimarães Netto, for help and guidance. Moreover, we thank the Coordenação de Aperfeiçoamento de Nível Superior (CAPES) for funding the scholarship.

References

Aarnes, I., Svensen, H., Connolly, J.A.D., Podladchikov, Y.Y.: How contact metamorphism can trigger global climate changes: Modeling gas generation around igneous sills in sedimentary basins. Geochim. Cosmochim. Acta 74, 7179–7195. https://doi.org/10.1016/j.gca.2010.09.011, 2010.

Aarnes, I., Podladchikov, Y., Svensen, H.: Devolatilization-induced pressure build-up: Implications for reaction front movement and breccia pipe formation. Geofluids 12, 265–279. https://doi.org/10.1111/j.1468-8123.2012.00368.x, 2012.

Agirrezabala, L.M., Permanyer, A., Suárez-Ruiz, I., Dorronsoro, C.: Contact metamorphism of organic-rich mudstones and carbon release around a magmatic sill in the Basque-Cantabrian Basin, western Pyrenees. Org. Geochem. 69, 26–35. https://doi.org/10.1016/j.orggeochem.2014.01.014, 2014.

Al-Agha, M.R., Burley, S.D., Curtis, C.D., Esson, J.: Complex cementation textures and authigenic mineral assemblages in Recent concretions from the Lincolnshire Wash (east coast, UK) driven by Fe(0) to Fe(II) oxidation. J. Geol. Soc. London. 152, 157–171. https://doi.org/10.1144/gsjgs.152.1.0157, 1995.

Aleali, M., Rahimpour-Bonab, H., Moussavi-Harami, R., Jahani, D.: Environmental and sequence stratigraphic implications of anhydrite textures: A case from the Lower Triassic of the Central Persian Gulf. J. Asian Earth Sci. 75, 110–125.
780 https://doi.org/10.1016/j.jseaes.2013.07.017, 2013.

Alhaddad, M.S., Ahmed, H.A.M.: A Review of Magnesite Mineral and its Industrial Application 1–13., 2022.

Almeida, F.F.M. de.: Distribuição regional e relações tectônicas do magmatismo pós-paleozoico no brasil. Rev. Bras. Geociências 17, 325–349. https://doi.org/10.25249/0375-7536.1986325349, 1987.

Apolinarska, K., Pełechaty, M., Pukacz, A.: CaCO3 sedimentation by modern charophytes (Characeae): can calcified remains
785 and carbonate δ13C and δ18O record the ecological state of lakes? – a review. Stud. Limnol. Telmatologica 5, 55–66, 2011.

Aquino, C.D., Buso, V.V., Faccini, U.F., Milana, J.P., Paim, P.S.G.: Facies and depositional architecture according to a jet efflux model of a late Paleozoic tidewater grounding-line system from the Itararé Group (Paraná Basin), southern Brazil. J. South Am. Earth Sci. 67, 180–200. https://doi.org/10.1016/j.jsames.2016.02.008, 2016.

Arp, G., Bissett, A., Brinkmann, N., Cousin, S., Beer, D.D.E., Friedl, T., Mohr, K.I., Neu, T.R., Reimer, A., Shiraishi, F.,
790 Stackebrandt, E., Zippel, B.: Tufa-forming biofilms of German karstwater streams: microorganisms, exopolymers, hydrochemistry and calcification. Microb. Phys. Control. 83–118, 2010.

Ayllón-Quevedo, F., Souza-Egipsy, V., Sanz-Montero, M.E., Rodríguez-Aranda, J.P.: Fluid inclusion analysis of twinned selenite gypsum beds from the Miocene of the Madrid basin (Spain). Implication on dolomite bioformation. Sediment. Geol. 201, 212–230. https://doi.org/10.1016/j.sedgeo.2007.06.001, 2007.

795 Bąbel, M.: Models for evaporite, selenite and gypsum microbialite deposition in ancient saline basins. Acta Geol. Pol. 54, 219–249, 2004.

Bąbel, M. Depositional environments of a salina-type evaporite basin recorded in the Badenian gypsum facies in the northern Carpathian Foredeep. Geol. Soc. London, Spec. Publ. 285, 107–142. https://doi.org/10.1144/SP285.7, 2007.

Balistieri, P. R. M. N., Netto, R. G., & Lavina, E. L. C.: Ichnofauna from the Upper Carboniferous-Lower Permian rhythmites
800 from Mafra, Santa Catarina State, Brazil: ichnotaxonomy. Revista Brasileira de Paleontologia, 4, 13-26, 2002.

Balistieri, P., Netto, R.G., Lavina, E.L.C.: Icnofauna de ritmitos do topo da Formação Mafra (Permo-Carbonífero da Bacia do Paraná) em Rio Negro, Estado do Paraná (PR), Brasil. Asoc. Paleontológica Argentina. IV Reun. Argentina Icnología y II Reun. Icnología del Mercosur 9, 131–139., 2003.

Balistieri, P., Netto, R.G., Sedorko, D.: Paleoichnology of the Itararé Group in the State of Santa Catarina and Rio Negro City
805 (PR), Brazil: a revision. Terr Plur. 15, e2118322. https://doi.org/10.5212/TerraPlural.v.15.2118322.039, 2021.

Baucon, A., De Carvalho, C.N., Felletti, F., Cabella, R.: Ichnofossils, cracks or crystals? A test for biogenicity of stick-like structures from vera rubin ridge, mars. Geosci. 10. https://doi.org/10.3390/geosciences10020039, 2020.

Beavington-Penney, S.J., Paul Wright, V., Woelkerling, W.J.: Recognising macrophyte-vegetated environments in the rock record: a new criterion using 'hooked' forms of crustose coralline red algae. Sediment. Geol. 166, 1–9.
810 https://doi.org/10.1016/j.sedgeo.2003.11.022, 2004.

Bengtson, S., Rasmussen, B., Ivarsson, M., Muhling, J., Broman, C., Marone, F., Stampanoni, M., Bekker, A.: Fungus-like mycelial fossils in 2.4-billion-year-old vesicular basalt. Nat. Ecol. Evol. 1, 1–6. https://doi.org/10.1038/s41559-017-0141, 2017.

Benzerara, K., Bernard, S., Miot, J.: Mineralogical Identification of Traces of Life. pp. 123–144. https://doi.org/10.1007/978-3-319-96175-0_6, 2019.

Benzerara, K., Menguy, N.: Looking for traces of life in minerals. Comptes Rendus Palevol 8, 617–628. https://doi.org/10.1016/j.crpv.2009.03.006, 2009.

Bindschedler, S., Cailleau, G., Braissant, O., Millière, L., Job, D., Verrecchia, E.P.: Unravelling the enigmatic origin of calcitic nanofibres in soils and caves: Purely physicochemical or biogenic processes? Biogeosciences 11, 2809–2825. https://doi.org/10.5194/bg-11-2809-2014, 2014.

Bindschedler, S., Cailleau, G., Verrecchia, E.: Role of Fungi in the Biomineralization of Calcite. Minerals 6, 41. https://doi.org/10.3390/min6020041, 2016.

Birgenheier, L.P., Fielding, C.R., Rygel, M.C., Frank, T.D., Roberts, J.: Evidence for Dynamic Climate Change on Sub-106-Year Scales from the Late Paleozoic Glacial Record, Tamworth Belt, New South Wales, Australia. J. Sediment. Res. 79, 56–82. https://doi.org/10.2110/jsr.2009.013, 2009.

Bontognali, T.R.R., Vasconcelos, C., Warthmann, R.J., Bernasconi, S.M., Dupraz, C., StrohmengeR, C.J., McKenzie, J.A.: Dolomite formation within microbial mats in the coastal sabkha of Abu Dhabi (United Arab Emirates). Sedimentology 57, 824–844. https://doi.org/10.1111/j.1365-3091.2009.01121.x, 2010.

Bosak, T., Newman, D.K.: Microbial Kinetic Controls on Calcite Morphology in Supersaturated Solutions. J. Sediment. Res. 75, 190–199. https://doi.org/10.2110/jsr.2005.015, 2005.

Botta, O., Bada, J.L., Gomez-Elvira, J., Javaux, E., Selsis, F., Summons, R.: Strategies of Life Detection, Springer Science & Business Media, Space Sciences Series of ISSI. Springer US, Boston, MA. https://doi.org/10.1007/978-0-387-77516-6, 2008.

Bower, D.M., Hummer, D.R., Steele, A., Kyono, A.: The Co-Evolution of Fe-Oxides, Ti-Oxides, and Other Microbially Induced Mineral Precipitates In.: Sandy Sediments: Understanding the Role of Cyanobacteria In Weathering and Early Diagenesis. J. Sediment. Res. 85, 1213–1227. https://doi.org/10.2110/jsr.2015.76, 2015.

Brace, W.F.: Permeability of crystalline and argillaceous rocks. Int. J. Rock Mech. Min. Sci. Geomech. 17, 241–251. https://doi.org/10.1016/0148-9062(80)90807-4, 1980.

Brasier, M., Green, O., Lindsay, J., Steele, A.: Earth's Oldest (~ 3.5 Ga) Fossils and the `Early Eden Hypothesis': Questioning the Evidence. Orig. Life Evol. Biosph. 34, 257–269. https://doi.org/10.1023/B:ORIG.0000009845.62244.d3, 2004.

Brasier, M.D., Green, O.R., Jephcoat, A.P., Kleppe, A.K., Van Kranendonk, M.J., Lindsay, J.F., Steele, A., Grassineau, N. V. Questioning the evidence for Earth's oldest fossils. Nature 416, 76–81. https://doi.org/10.1038/416076a, 2002.

Brasier, M.D., Wacey, D. Fossils and astrobiology: new protocols for cell evolution in deep time. Int. J. Astrobiol. 11, 217–228. https://doi.org/10.1017/S1473550412000298, 2012.

Briggs, D.E.G.: The Role of Decay and Mineralization in the Preservation of Soft-Bodied Fossils. Annu. Rev. Earth Planet.

845   Sci. 31, 275–301. https://doi.org/10.1146/annurev.earth.31.100901.144746, 2003.

Briggs, D.E.G., McMahon, S.: The role of experiments in investigating the taphonomy of exceptional preservation. Palaeontology 59, 1–11. https://doi.org/10.1111/pala.12219, 2016.

Buatois, L.A., Netto, R.G., Mángano, M.G., Balistieri, P.R.M.N.^: Extreme freshwater release during the late Paleozoic Gondwana deglaciation and its impact on coastal ecosystems. Geology 34, 1021. https://doi.org/10.1130/G22994A.1, 2006.

850   Buick, R.: Microfossil Recognition in Archean Rocks: An Appraisal of Spheroids and Filaments from a 3500 M.Y. Old Chert-Barite Unit at North Pole, Western Australia. Palaios 5, 441. https://doi.org/10.2307/3514837, 1990.

Burley, S., Worden, R.: Sandstone Diagenesis: Recent and Ancient, International Association Of Sedimentologists Reprints. , 2003.

Burley, S.D., Kantorowicz, J.D., Waugh, B.: Clastic diagenesis. Geol. Soc. London, Spec. Publ. 18, 189–226.

855   https://doi.org/10.1144/GSL.SP.1985.018.01.10, 1985.

Cagliari, J., Philipp, R.P., Buso, V.V., Netto, R.G., Klaus Hillebrand, P., da Cunha Lopes, R., Stipp Basei, M.A., Faccini, U.F.: Age constraints of the glaciation in the Paraná Basin: evidence from new U–Pb dates. J. Geol. Soc. London. 173, 871–874. https://doi.org/10.1144/jgs2015-161, 2016.

Cailleau, G., Verrecchia, E.P., Braissant, O., Emmanuel, L.: The biogenic origin of needle fibre calcite. Sedimentology 56,

860   1858–1875. https://doi.org/10.1111/j.1365-3091.2009.01060.x, 2009.

Callefo, Flavia, Maldanis, L., Teixeira, V.C., Abans, R.A. de O., Monfredini, T., Rodrigues, F., Galante, D. Evaluating Biogenicity on the Geological Record with Synchrotron-Based Techniques. Front. Microbiol. 10, 1–12. https://doi.org/10.3389/fmicb.2019.02358, 2019.

Callefo, F., Ricardi-Branco, F., Hartmann, G.A., Galante, D., Rodrigues, F., Maldanis, L., Yokoyama, E., Teixeira, V.C.,

865   Noffke, N., Bower, D.M., Bullock, E.S., Braga, A.H., Coaquira, J.A.H., Fernandes, M.A.: Evaluating iron as a biomarker of rhythmites — An example from the last Paleozoic ice age of Gondwana. Sediment. Geol. 383, 1–15. https://doi.org/10.1016/j.sedgeo.2019.02.002, 2019.

Canuto, J.R., dos Santos, P.R., & Rocha-Campos, A.C.: Estratigrafia de sequênicas do grupo Itararé (Neopaleozoico). Revista Brasileira de Geociências, 31(1), 107-116, 2001

870   Cardoso, A.R., Basilici, G., da Silva, P.A.S.: Early diagenetic calcite replacement of evaporites in playa lakes of the Quiricó Formation (Lower Cretaceous, SE Brazil). Sediment. Geol. 438. https://doi.org/10.1016/j.sedgeo.2022.106212, 2022.

Daemon, R. F., & Quadros, L. D.: Bioestratigrafia do Neopaleozóico da bacia do Paraná. In: Congresso Brasileiro de Geologia, 24, 359-412, 1970.

Davies, G.R., Smith, L.B.: Structurally controlled hydrothermal dolomite reservoir facies: An overview. Am. Assoc. Pet. Geol.

875   Bull. 90, 1641–1690. https://doi.org/10.1306/05220605164, 2006.

Davies, N.S., Liu, A.G., Gibling, M.R., Miller, R.F.: Resolving MISS conceptions and misconceptions: A geological approach to sedimentary surface textures generated by microbial and abiotic processes. Earth-Science Rev. 154, 210–246. https://doi.org/10.1016/j.earscirev.2016.01.005, 2016.

Davies, N.S., Shillito, A.P., Slater, B.J., Liu, A.G., McMahon, W.J.: Evolutionary synchrony of Earth's biosphere and sedimentary-stratigraphic record. Earth-Science Rev. 201, 102979. https://doi.org/10.1016/j.earscirev.2019.102979, 2020.

de Barros, G.E.B., Becker-Kerber, B., Sedorko, D., Lima, J.H.D., Pacheco, M.L.A.F.: Ichnological aspects of the Aquidauana Formation (Upper Carboniferous, Itararé Group, Brazil): An arthropod-colonized glacial setting. Palaeogeogr. Palaeoclimatol. Palaeoecol. 578, 110575. https://doi.org/10.1016/j.palaeo.2021.110575, 2021.

De Vargas, T., Boff, F.E., Belladona, R., Faccioni, L.F., Reginato, P.A.R., Carlos, F.S.: Influence of geological discontinuities on the groundwater flow of the Serra Geral Fractured Aquifer System. Groundw. Sustain. Dev. 18, 100780. https://doi.org/10.1016/j.gsd.2022.100780, 2022.

Della Porta, G.: Carbonate build-ups in lacustrine, hydrothermal and fluvial settings: comparing depositional geometry, fabric types and geochemical signature. Geol. Soc. London, Spec. Publ. 418, 17–68. https://doi.org/10.1144/SP418.4, 2015.

Dodd, M.S., Papineau, D., Grenne, T., Slack, J.F., Rittner, M., Pirajno, F., O'Neil, J., Little, C.T.S.: Evidence for early life in Earth's oldest hydrothermal vent precipitates. Nature 543, 60–64. https://doi.org/10.1038/nature21377, 2017.

Douglas, S., Beveridge, T.: Mineral formation by bacteria in natural microbial communities. FEMS Microbiol. Ecol. 26, 79–88. https://doi.org/10.1016/S0168-6496(98)00027-0, 1998.

Dupraz, C., Visscher, P.T., Baumgartner, L.K., Reid, R.P.: Microbe-mineral interactions: early carbonate precipitation in a hypersaline lake (Eleuthera Island, Bahamas). Sedimentology 51, 745–765. https://doi.org/10.1111/j.1365-3091.2004.00649.x, 2004.

Dupraz, C., Reid, R.P., Braissant, O., Decho, A.W., Norman, R.S., Visscher, P.T.: Processes of carbonate precipitation in modern microbial mats. Earth-Science Rev. 96, 141–162. https://doi.org/10.1016/j.earscirev.2008.10.005, 2009.

Eugster, H.P.: Geochemistry of Evaporitic Lacustrine Deposits. Annu. Rev. Earth Planet. Sci. 8, 35–63. https://doi.org/10.1146/annurev.ea.08.050180.000343, 1980.

Eymard, I., Alvarez, M., Bilmes, A., Vasconcelos, C., Ariztegui, D.: Tracking Organomineralization Processes from Living Microbial Mats to Fossil Microbialites. Minerals 10, 605. https://doi.org/10.3390/min10070605, 2020.

Farias, F., Szatmari, P., Bahniuk, A., França, A.B.: Evaporitic carbonates in the pre-salt of Santos Basin – Genesis and tectonic implications. Mar. Pet. Geol. 105, 251–272. https://doi.org/10.1016/j.marpetgeo.2019.04.020, 2019.

Finkelman, R.B., Bostick, N.H., Dulong, F.T., Senftle, F.E., Thorpe, A.N.: Influence of an igneous intrusion on the inorganic geochemistry of a bituminous coal from Pitkin County, Colorado. Int. J. Coal Geol. 36, 223–241. https://doi.org/10.1016/S0166-5162(98)00005-6, 1998.

Franca, A.B., Potter, P.E.: Estratigrafia, ambiente deposicional e análise de reservatório do Grupo Itararé (Permocarbonifero), Bacia do Parana (Parte 1). Bol. Geociencias - Petrobras 2, 147–191, 1988.

Frank, H.T., Gomes, M.E.B., Formoso, M.L.L.: Revisão da extensão areal e do volume da Formação Serra Geral, Bacia do
Paraná, América do Sul. Pesqui. em Geociências 36, 49. https://doi.org/10.22456/1807-9806.17874, 2009.

Gandini, R., Netto, R.G., Souza, P.A.: Paleoicnologia e a palinologia dos ritmitos do Grupo Itararé na pedreira de Águas Claras
(Santa Catarina , Brasil). Gaea 3, 47–59., 2007.

Garber, R.A., Levy, Y., Friedman, G.M.: The sedimentology of the Dead Sea. Carbonates and Evaporites 2, 43–57.
https://doi.org/10.1007/BF03174303, 1987.

García Ruiz, J.M., Carnerup, A., Christy, A.G., Welham, N.J., Hyde, S.T.: Morphology: An Ambiguous Indicator of
Biogenicity. Astrobiology 2, 353–369. https://doi.org/10.1089/153110702762027925, 2002.

Gargaud, M., Irvine, W.M., Amils, R., Cleaves, H.J., Pinti, D.L., Quintanilla, J.C., Rouan, D., Spohn, T., Tirard, S., Viso, M.
(Eds.) Encyclopedia of Astrobiology. Springer Berlin Heidelberg, Berlin, Heidelberg. https://doi.org/10.1007/978-3-662-
44185-5, 2015.

Golab, A.N., Hutton, A.C., French, D.: Petrography, carbonate mineralogy and geochemistry of thermally altered coal in
Permian coal measures, Hunter Valley, Australia. Int. J. Coal Geol. 70, 150–165. https://doi.org/10.1016/j.coal.2006.01.010,
2007.

Golubic, S., Seong-Joo, L., Browne, K.M.: Cyanobacteria: Architects of Sedimentary Structures, in: Microbial Sediments.
Springer Berlin Heidelberg, Berlin, Heidelberg, pp. 57–67. https://doi.org/10.1007/978-3-662-04036-2_8, 2000.

Gomes, A.L.S., Becker-Kerber, B., Osés, G.L., Prado, G., Becker Kerber, P., de Barros, G.E.B., Galante, D., Rangel, E.,
Bidola, P., Herzen, J., Pfeiffer, F., Rizzutto, M.A., Pacheco, M.L.A.F.: Paleometry as a key tool to deal with paleobiological
and astrobiological issues: some contributions and reflections on the Brazilian fossil record. Int. J. Astrobiol. 18, 575–589.
https://doi.org/10.1017/S1473550418000538, 2019.

Granier, B.: The contribution of calcareous green algae to the production of limestones: a review. Geodiversitas 34, 35–60.
https://doi.org/10.5252/g2012n1a3, 2012.

Green, S.: Polymerized Tubular Silicates in Lower Cambrian Carbonates – Biology or Chemistry?, 2022.

Grgasović, T.: Taxonomy of the fossil calcareous algae: Revision of genera Physoporella Steinmann and Oligoporella Pia
(Dasycladales). Carnets géologie (Notebooks Geol. 22, 171–310. https://doi.org/10.2110/carnets.2022.2207, 2022.

Hartmann, L.A., da Cunha Duarte, L., Massonne, H.-J., Michelin, C., Rosenstengel, L.M., Bergmann, M., Theye, T., Pertille,
J., Arena, K.R., Duarte, S.K., Pinto, V.M., Barboza, E.G., Rosa, M.L.C.C., Wildner, W.: Sequential opening and filling of
cavities forming vesicles, amygdales and giant amethyst geodes in lavas from the southern Paraná volcanic province, Brazil
and Uruguay. Int. Geol. Rev. 54, 1–14. https://doi.org/10.1080/00206814.2010.496253, 2012.

Hellevang, H., Aagaard, P., Jahren, J.: Will dawsonite form during CO 2 storage? Greenh. Gases Sci. Technol. 4, 191–199.
https://doi.org/10.1002/ghg.1378, 2014.

Hofman, H. J.: Precambrian remains in Canada: fossils, dubiofossils, and pseudofossils. In: Proceedings of the 24th
International Geological Congress, Section. 20-30, 1972.

Hofmann, H.J.: Archean Microfossils and Abiomorphs. Astrobiology 4, 135–136. https://doi.org/10.1089/153110704323175115, 2004.

Hooper, J.N.A., Van Soest, R.W.M.: Systema Porifera. A Guide to the Classification of Sponges, in: Systema Porifera. Springer US, pp. 1–7. https://doi.org/10.1007/978-1-4615-0747-5_1, 2002.

Huntington, K.W., Budd, D.A., Wernicke, B.P., Eiler, J.M.: Use of Clumped-Isotope Thermometry To Constrain the Crystallization Temperature of Diagenetic Calcite. J. Sediment. Res. 81, 656–669. https://doi.org/10.2110/jsr.2011.51, 2011.

Inglez, L., Warren, L. V., Quaglio, F., Netto, R.G., Okubo, J., Arrouy, M.J., Simões, M.G., Poiré, D.G.: Scratching the discs: evaluating alternative hypotheses for the origin of the Ediacaran discoidal structures from the Cerro Negro Formation, La Providencia Group, Argentina. Geol. Mag. 159, 1192–1209. https://doi.org/10.1017/S0016756821000327, 2021.

Isbell, J.L., Miller, M.F., Wolfe, K.L., Lenaker, P.A.: Timing of late Paleozoic glaciation in Gondwana: Was glaciation responsible for the development of Northern Hemisphere cyclothems?, in: Extreme Depositional Environments: Mega End Members in Geologic Time. Geological Society of America, pp. 5–24. https://doi.org/10.1130/0-8137-2370-1.5, 2003.

Ivarsson, M., Drake, H., Neubeck, A., Sallstedt, T., Bengtson, S., Roberts, N.M.W., Rasmussen, B.: The fossil record of igneous rock. Earth-Science Rev. 210, 103342. https://doi.org/10.1016/j.earscirev.2020.103342, 2020.

Ivarsson, M., Drake, H., Neubeck, A., Snoeyenbos-West, O., Belivanova, V., Bengtson, S.: Introducing palaeolithobiology. GFF 143, 305–319. https://doi.org/10.1080/11035897.2021.1895302, 2021.

Kisch, H.J., Taylor, G.H.: Metamorphism and alteration near an intrusive-coal contact. Econ. Geol. 61, 343–361. https://doi.org/10.2113/gsecongeo.61.2.343, 1966.

Knoll, A.H.: Systems paleobiology. Geol. Soc. Am. Bull. 125, 3–13. https://doi.org/10.1130/B30685.1, 2013.

Kraus, E.A., Beeler, S.R., Mors, R.A., Floyd, J.G., Stamps, B.W., Nunn, H.S., Stevenson, B.S., Johnson, H.A., Shapiro, R.S., Loyd, S.J., Spear, J.R., Corsetti, F.A.: Microscale biosignatures and abiotic mineral authigenesis in Little Hot Creek, California. Front. Microbiol. 9, 1–13. https://doi.org/10.3389/fmicb.2018.00997, 2018.

Kropp, J., Von Bloh, W., Klenke, T.: Calcite formation in microbial mats: Modeling and quantification of inhomogeneous distribution patterns by a cellular automaton model and multifractal measures. Int. J. Earth Sci. 85, 857–863. https://doi.org/10.1007/s005310050117, 1996.

Kropp, J., Block, A., Von Bloh, W., Klenke, T., Schellnhuber, H.J.: Multifractal characterization of microbially induced magnesian calcite formation in recent tidal flat sediments. Sediment. Geol. 109, 37–51. https://doi.org/10.1016/S0037-0738(96)00059-0, 1997.

Kunoh, T., Hashimoto, H., McFarlane, I.R., Hayashi, N., Suzuki, T., Taketa, E., Tamura, K., Takano, M., El-Naggar, M.Y., Kunoh, H., Takada, J., 2016. Abiotic deposition of Fe complexes onto Leptothrix sheaths. Biology (Basel). 5. https://doi.org/10.3390/biology5020026

Leonov, M. V, Fedonkin, M.A.: Discovery of the first macroscopic algal assemblage in the Terminal Proterozoic of Namibia, southwest Africa. Commun. Geol. Surv. Namib 14, 87–93, 2009.

975   Lepot, K., Addad, A., Knoll, A.H., Wang, J., Troadec, D., Béché, A., Javaux, E.J.: Iron minerals within specific microfossil morphospecies of the 1.88 Ga Gunflint Formation. Nat. Commun. 8. https://doi.org/10.1038/ncomms14890, 2017.

Lerner, A.J., Lucas, S.G.: Gallery of geology: The rare and unusual pseudofossil Astropolithon from the lower permian abo formation near Socorro, New Mexico. New Mex. Geol. 39, 40–42, 2017.

Lima, J.H.D., Netto, R.G., Corrêa, C.G., Lavina, E.L.C.: Ichnology of deglaciation deposits from the Upper Carboniferous Rio
980   do Sul Formation (Itararé Group, Paraná Basin) at central-east Santa Catarina State (southern Brazil). J. South Am. Earth Sci. 63, 137–148. https://doi.org/10.1016/j.jsames.2015.07.008, 2015.

Lima, J.H.D., Minter, N.J., Netto, R.G.: Insights from functional morphology and neoichnology for determining tracemakers: a case study of the reconstruction of an ancient glacial arthropod-dominated fauna. Lethaia 50, 576–590. https://doi.org/10.1111/let.12214, 2017.

985   Lin, C.Y., Turchyn, A. V., Krylov, A., Antler, G.: The microbially driven formation of siderite in salt marsh sediments. Geobiology 18, 207–224. https://doi.org/10.1111/gbi.12371, 2020.

Lippmann, F.: Sedimentary Carbonate Minerals. Springer Berlin Heidelberg, Berlin, Heidelberg. https://doi.org/10.1007/978-3-642-65474-9, 1973.

Liu, C., Xie, Q., Wang, G., Zhang, C., Wang, L., Qi, K.: Reservoir properties and controlling factors of contact metamorphic
990   zones of the diabase in the northern slope of the Gaoyou Sag, Subei Basin, eastern China. J. Nat. Gas Sci. Eng. 35, 392–411. https://doi.org/10.1016/j.jngse.2016.08.070, 2016.

Loope, D.B.: Rhizoliths in ancient eolianites. Sediment. Geol. 56, 301–314. https://doi.org/10.1016/0037-0738(88)90058-9, 1988.

Lu, Z., Rickaby, R.E.M., Kennedy, H., Kennedy, P., Pancost, R.D., Shaw, S., Lennie, A., Wellner, J., Anderson, J.B.: An ikaite
995   record of late Holocene climate at the Antarctic Peninsula. Earth Planet. Sci. Lett. 325–326, 108–115. https://doi.org/10.1016/j.epsl.2012.01.036, 2012.

Maiklem, W. R., Bebout, D. G., Glaister, R. P.: Classification of anhydrite—practical approach. Bulletin of Canadian Petroleum Geology, 17(2), 194-233, 1969

Makovicky, E., Karup-Møller, S., Li, J.: Mineralogy of the chrysanthemum stone. Neues Jahrb. für Mineral. - Abhandlungen
1000   182, 241–251. https://doi.org/10.1127/0077-7757/2006/0048, 2006.

Maldanis, L., Hickman-Lewis, K., Verezhak, M., Gueriau, P., Guizar-Sicairos, M., Jaqueto, P., Trindade, R.I.F., Rossi, A.L., Berenguer, F., Westall, F., Bertrand, L., Galante, D.: Nanoscale 3D quantitative imaging of 1.88 Ga Gunflint microfossils reveals novel insights into taphonomic and biogenic characters. Sci. Rep. 10, 8163. https://doi.org/10.1038/s41598-020-65176-w, 2020.

1005   Maliva, R.G.: Displacive Calcite Syntaxial Overgrowths in Open Marine Limestones. SEPM J. Sediment. Res. Vol. 59, 397–403. https://doi.org/10.1306/212F8FA3-2B24-11D7-8648000102C1865D, 1989.

Martins, A.K., Kerkhoff, M.L.H., Dutra, T.L., Horodyski, R.S., Kochhann, K.G.D., Forancelli Pacheco, M.L.A.: Exceptional preservation of Triassic-Jurassic fossil plants: integrating biosignatures and fossil diagenesis to understand microbial-related iron dynamics. Lethaia 55, 1–16. https://doi.org/10.18261/let.55.3.4, 2022.

1010   Mason, R., Burton, K.W., Yuan, Y., She, Z.: Chiastolite. Gondwana Res. 18, 222–229. https://doi.org/10.1016/j.gr.2010.03.005, 2010.

Mason, R., Liu, R.: The Origin of Spots in Contact Aureoles and Over-Heating of Country Rock Next to a Dyke. J. Earth Sci. 29, 1005–1009. https://doi.org/10.1007/s12583-018-0882-5, 2018.

McLoughlin, N., Grosch, E.G.: A Hierarchical System for Evaluating the Biogenicity of Metavolcanic- and Ultramafic-Hosted

1015   Microalteration Textures in the Search for Extraterrestrial Life. Astrobiology 15, 901–921. https://doi.org/10.1089/ast.2014.1259, 2015.

McMahon, S., Cosmidis, J.: False biosignatures on Mars: anticipating ambiguity. J. Geol. Soc. London. 179. https://doi.org/10.1144/jgs2021-050, 2022.

McMahon, S., Ivarsson, M.: A New Frontier for Palaeobiology: Earth's Vast Deep Biosphere. BioEssays 41, 1900052.

1020   https://doi.org/10.1002/bies.201900052, 2019.

McMahon, S., Ivarsson, M., Wacey, D., Saunders, M., Belivanova, V., Muirhead, D., Knoll, P., Steinbock, O., Frost, D.A.: Dubiofossils from a Mars-analogue subsurface palaeoenvironment: The limits of biogenicity criteria. Geobiology 19, 473–488. https://doi.org/10.1111/gbi.12445, 2021.

Merino, N., Aronson, H.S., Bojanova, D.P., Feyhl-Buska, J., Wong, M.L., Zhang, S., Giovannelli, D.: Living at the Extremes:

1025   Extremophiles and the Limits of Life in a Planetary Context. Front. Microbiol. 10. https://doi.org/10.3389/fmicb.2019.00780, 2019.

Meyers, P.A., Simoneit, B.R.T.: Effects of extreme heating on the elemental and isotopic compositions of an Upper Cretaceous coal. Org. Geochem. 30, 299–305. https://doi.org/10.1016/S0146-6380(99)00015-7, 1999.

Milani, E.J., Melo, J.H.G. De, Souza, P.A. De, Fernandes, L.A., França, A.B.: Bacia do Paraná, Boletim de Geociências da

1030   PETROBRAS, v. 15. 265–287, 2007.

Monroe, J.S., Dietrich, R. V.: Pseudofossils. Rocks Miner. 65, 150–158. https://doi.org/10.1080/00357529.1990.11761667, 1990.

Mücke, A.: Chamosite, siderite and the environmental conditions of their formation in chamosite-type Phanerozoic ooidal ironstones. Ore Geol. Rev. 28, 235–249. https://doi.org/10.1016/j.oregeorev.2005.03.004, 2006.

1035   Müller, W.E.G., Belikov, S.I., Tremel, W., Perry, C.C., Gieskes, W.W.C., Boreiko, A., Schröder, H.C.: Siliceous spicules in marine demosponges (example Suberites domuncula). Micron 37, 107–120. https://doi.org/10.1016/j.micron.2005.09.003, 2006.

Muscente, A.D., Schiffbauer, J.D., Broce, J., Laflamme, M., O'Donnell, K., Boag, T.H., Meyer, M., Hawkins, A.D., Huntley, J.W., McNamara, M., MacKenzie, L.A., Stanley, G.D., Hinman, N.W., Hofmann, M.H., Xiao, S.: Exceptionally preserved

1040   fossil assemblages through geologic time and space. Gondwana Res. 48, 164–188. https://doi.org/10.1016/j.gr.2017.04.020, 2017.

Nardy, A. J. R., Oliveira, M. D., Betancourt, R. H. S., Verdugo, D. R. H., & Machado, F. B.: Geologia e estratigrafia da Formação Serra geral. Geociências, 21(1), 15-32, 2002

Netto, R.G., Balistieri, P.R.M.N., Lavina, E.L.C., Silveira, D.M.: Ichnological signatures of shallow freshwater lakes in the

1045   glacial Itararé Group (Mafra Formation, Upper Carboniferous–Lower Permian of Paraná Basin, S Brazil). Palaeogeogr. Palaeoclimatol. Palaeoecol. 272, 240–255. https://doi.org/10.1016/j.palaeo.2008.10.028, 2009.

Netto, R.G., Corrêa, C.G., Lima, J.H.D., Sedorko, D., Villegas-Martín, J.: Deciphering myriapoda population dynamics during Gondwana deglaciation cycles through neoichnology. J. South Am. Earth Sci. 109. https://doi.org/10.1016/j.jsames.2021.103247, 2021.

1050   Neveu, M., Hays, L.E., Voytek, M.A., New, M.H., Schulte, M.D.: The Ladder of Life Detection. Astrobiology 18, 1375–1402. https://doi.org/10.1089/ast.2017.1773, 2018.

Noffke, N.: The criteria for the biogeneicity of microbially induced sedimentary structures (MISS) in Archean and younger, sandy deposits. Earth-Science Rev. 96, 173–180. https://doi.org/10.1016/j.earscirev.2008.08.002, 2009.

Noffke, N.: Geobiology. Springer Berlin Heidelberg, Berlin, Heidelberg. https://doi.org/10.1007/978-3-642-12772-4, 2010.

1055   Noffke, N.: Comment on the paper by Davies et al. "Resolving MISS conceptions and misconceptions: A geological approach to sedimentary surface textures generated by microbial and abiotic processes" (Earth Science Reviews, 154 (2016), 210–246). Earth-Science Rev. 176, 373–383. https://doi.org/10.1016/j.earscirev.2017.11.021, 2018.

Noffke, N.: Microbially Induced Sedimentary Structures in Clastic Deposits: Implication for the Prospection for Fossil Life on Mars. Astrobiology 21, 866–892. https://doi.org/10.1089/ast.2021.0011, 2021.

1060   Noffke, N., Gerdes, G., Klenke, T., Krumbein, W.E.: A microscopic sedimentary succession of graded sand and microbial mats in modern siliciclastic tidal flats. Sediment. Geol. 110, 1–6. https://doi.org/10.1016/S0037-0738(97)00039-0, 1997.

Noffke, N., Gerdes, G., Klenke, T., Krumbein, W.E.: Microbially Induced Sedimentary Structures--A New Category Within the Classification of Primary Sedimentary Structures--Reply. J. Sediment. Res. 72, 589–590. https://doi.org/10.1306/010302720589, 2001.

1065   Noffke, N., Knoll, A.H., Grotzinger, J.P.: Sedimentary Controls on the Formation and Preservation of Microbial Mats in Siliciclastic Deposits: A Case Study from the Upper Neoproterozoic Nama Group, Namibia. Palaios 17, 533–544. https://doi.org/10.1669/0883-1351(2002)017<0533:SCOTFA>2.0.CO;2, 2002.

Noll, S.H., Netto, R.G.: Microbially induced sedimentary structures in late Pennsylvanian glacial settings: A case study from the Gondwanan Paraná Basin. J. South Am. Earth Sci. 88, 385–398. https://doi.org/10.1016/j.jsames.2018.09.010, 2018.

1070   Payandi-Rolland, Roche, Vennin, Visscher, Amiotte-Suchet, Thomas, Bundeleva: Carbonate Precipitation in Mixed Cyanobacterial Biofilms Forming Freshwater Microbial Tufa. Minerals 9, 409. https://doi.org/10.3390/min9070409, 2019.

Perillo, V.L., Maisano, L., Martinez, A.M., Quijada, I.E., Cuadrado, D.G.: Microbial mat contribution to the formation of an evaporitic environment in a temperate-latitude ecosystem. J. Hydrol. 575, 105–114. https://doi.org/10.1016/j.jhydrol.2019.05.027, 2019.

1075   Pitra, P., De Waal, S.A.: High-temperature, low-pressure metamorphism and development of prograde symplectites, Marble Hall Fragment, Bushveld Complex (South Africa). J. Metamorph. Geol. 19, 311–325. https://doi.org/10.1046/j.1525-1314.2001.00313.x, 2001.

Porada, H., Ghergut, J., Bouougri, E.H.: Kinneyia-Type Wrinkle Structures--Critical Review and Model Of Formation. Palaios 23, 65–77. https://doi.org/10.2110/palo.2006.p06-095r, 2008.

1080   Pratt, B.R.: Calcification of cyanobacterial filaments: Girvanella and the origin of lower Paleozoic lime mud. Geology 29, 763. https://doi.org/10.1130/0091-7613(2001)029<0763:COCFGA>2.0.CO;2, 2001.

Puigdomenech, C.G., Carvalho, B., Paim, P.S.G., Faccini, U.F.: Lowstand Turbidites and Delta Systems of the Itararé Group in the Vidal Ramos region (SC), southern Brazil. Brazilian J. Geol. 44, 529–544. https://doi.org/10.5327/Z23174889201400040002, 2014.

1085   Purgstaller, B., Dietzel, M., Baldermann, A., Mavromatis, V.: Control of temperature and aqueous Mg2+/Ca2+ ratio on the (trans-)formation of ikaite. Geochim. Cosmochim. Acta 217, 128–143. https://doi.org/10.1016/j.gca.2017.08.016, 2017.

Reijmer, J.J.G.: Marine carbonate factories: Review and update. Sedimentology 68, 1729–1796. https://doi.org/10.1111/sed.12878, 2021.

Ren, M., Jones, B.: Modern authigenic amorphous and crystalline iron oxyhydroxides in subsurface Ordovician dolostones

1090   (Jinan, North China Block): Biomineralization and crystal morphology. Sediment. Geol. 426, 106044. https://doi.org/10.1016/j.sedgeo.2021.106044, 2021.

Roberts, J.A., Bennett, P.C., González, L.A., Macpherson, G.L., Milliken, K.L.: Microbial precipitation of dolomite in methanogenic groundwater. Geology 32, 277. https://doi.org/10.1130/G20246.2, 2004.

Roden, E.E., Kappler, A., Bauer, I., Jiang, J., Paul, A., Stoesser, R., Konishi, H., Xu, H.: Extracellular electron transfer through

1095   microbial reduction of solid-phase humic substances. Nat. Geosci. 3, 417–421. https://doi.org/10.1038/ngeo870, 2010.

Rodriguez-Navarro, C., Jimenez-Lopez, C., Rodriguez-Navarro, A., Gonzalez-Muñoz, M.T., Rodriguez-Gallego, M.: Bacterially mediated mineralization of vaterite. Geochim. Cosmochim. Acta 71, 1197–1213. https://doi.org/10.1016/j.gca.2006.11.031, 2007.

Rouillard, J., Van Zuilen, M., Pisapia, C., Garcia-Ruiz, J.M.: An Alternative Approach for Assessing Biogenicity. Astrobiology

1100   21, 151–164. https://doi.org/10.1089/ast.2020.2282, 2021.

Salamuni, R., Marques Filho, P. L., Sobanski, A. C.: Considerações sobre turbiditos da Formação Itararé (Carbonífero Superior), Rio Negro-PR e Mafra-SC. Boletim da Sociedade Brasileira de Geologia, 15, 1-19, 1966.

Salvany, J.M., García-Veigas, J., Ortí, F.: Glauberite-halite association of the Zaragoza Gypsum Formation (Lower Miocene, Ebro Basin, NE Spain). Sedimentology 54, 443–467. https://doi.org/10.1111/j.1365-3091.2006.00844.x, 2007.

1105 Sánchez-Navas, A., de Cassia Oliveira-Barbosa, R., García-Casco, A., Martín-Algarra, A., 2012. Transformation of Andalusite to Kyanite in the Alpujarride Complex (Betic Cordillera, Southern Spain): Geologic Implications. J. Geol. 120, 557–574. https://doi.org/10.1086/666944

Santos, R.V., Dantas, E.L., Oliveira, C.G. de, Alvarenga, C.J.S. de, Anjos, C.W.D. dos, Guimarães, E.M., Oliveira, F.B.: Geochemical and thermal effects of a basic sill on black shales and limestones of the Permian Irati Formation. J. South Am.
1110 Earth Sci. 28, 14–24. https://doi.org/10.1016/j.jsames.2008.12.002, 2009.

Saxby, J.D., Stephenson, L.C.: Effect of anigneous intrusion on oil shale at Rundle (Australia). Chem. Geol. 63, 1–16. https://doi.org/10.1016/0009-2541(87)90068-4, 1987

Schemiko, D.C.B., Vesely, F.F., Rodrigues, M.C.N.L.: Deepwater to fluvio-deltaic stratigraphic evolution of a deglaciated depocenter: The early Permian Rio do Sul and Rio Bonito formations, southern Brazil. J. South Am. Earth Sci. 95, 102260.
1115 https://doi.org/10.1016/j.jsames.2019.102260, 2019.

Schiffbauer, J.D., Yin, L., Bodnar, R.J., Kaufman, A.J., Meng, F., Hu, J., Shen, B., Yuan, X., Bao, H., Xiao, S.: Ultrastructural and Geochemical Characterization of Archean–Paleoproterozoic Graphite Particles: Implications for Recognizing Traces of Life in Highly Metamorphosed Rocks. Astrobiology 7, 684–704. https://doi.org/10.1089/ast.2006.0098, 2007.

Schneider, R., Mühlmann, H., Tommasi, E., Medeiros, R. D., Daemon, R. F., Nogueira, A. A.: Revisão estratigráfica da Bacia
1120 do Paraná. In Congresso brasileiro de Geologia. 28, 41-65, 1974.

Schopf, J.W.: Fossil evidence of Archaean life. Philos. Trans. R. Soc. B Biol. Sci. 361, 869–885. https://doi.org/10.1098/rstb.2006.1834, 2006.

Schopf, J.W., Kudryavtsev, A.B.: Biogenicity of Earth's earliest fossils: A resolution of the controversy. Gondwana Res. 22, 761–771. https://doi.org/10.1016/j.gr.2012.07.003, 2012.

1125 Schopf, J.W., Kudryavtsev, A.B., Agresti, D.G., Wdowiak, T.J., Czaja, A.D.: Schoopf et al., 2002 73–76. , 2002.

Schopf, J.W., Kudryavtsev, A.B., Czaja, A.D., Tripathi, A.B.: Evidence of Archean life: Stromatolites and microfossils. Precambrian Res. 158, 141–155. https://doi.org/10.1016/j.precamres.2007.04.009, 2007.

Schubert, C.J., Nürnberg, D., Scheele, N., Pauer, F., Kriews, M., 1997. 13 C isotope depletion in ikaite crystals: evidence for methane release from the Siberian shelves Geo-Marine Lett. 17, 169–174. https://doi.org/10.1007/s003670050023

1130 Schultz, B., Thibault, N., Huggett, J.: The minerals ikaite and its pseudomorph glendonite: Historical perspective and legacies of Douglas Shearman and Alec K. Smith. Proc. Geol. Assoc. https://doi.org/10.1016/j.pgeola.2022.02.003, 2022.

Sethmann, I., Wörheide, G.: Structure and composition of calcareous sponge spicules: A review and comparison to structurally related biominerals. Micron 39, 209–228. https://doi.org/10.1016/j.micron.2007.01.006, 2008.

Shearman, D.J., Mcgugan, A., Stein, C., Smith, A.J.: Ikaite, CaCO3·6H2O, precursor of the thinolites in the Quaternary tufas
1135 and tufa mounds of the Lahontan and Mono Lake Basins, western United States. Geol. Soc. Am. Bull. 101, 913–917. https://doi.org/10.1130/0016-7606(1989)101<0913:ICOPOT>2.3.CO;2 1989.

Sibley, D.F., Nordeng, S.H., Borkowski, M.L.: Dolomitization kinetics of hydrothermal bombs and natural settings. J. Sediment. Res. 64, 630–637. https://doi.org/10.1306/D4267E29-2B26-11D7-8648000102C1865D, 1994.

Silva, M.S., Uso de medidas digitais em RGB em fitoclastos na caracterização da influência térmica das intrusivas ígneas (Grupo Serra Geral) nos siltitos da Formação Taciba, Itaiópolis, SC. Undergraduate geology monograph, Universidade Federal de Santa Catarina, Florianópolis., 2020.

Slater, G.F.: Biosignatures: Interpreting Evidence of the Origins and Diversity of Life. Geosci. Canada 36, 170–178, 2009.

Sommer, V.P., Kuchle, J., De Ros, L.F.: Seismic stratigraphic framework and seismic facies of the Aptian Pre-salt Barra Velha Formation in the Tupi Field, Santos Basin, Brazil. J. South Am. Earth Sci. 118, 103947. https://doi.org/10.1016/j.jsames.2022.103947, 2022.

Souza, P.A.: Late Carboniferous palynostratigraphy of the Itararé Subgroup, northeastern Paraná Basin, Brazil. Rev. Palaeobot. Palynol. 138, 9–29. https://doi.org/10.1016/j.revpalbo.2005.09.004, 2006.

Spadafora, A., Perri, E., Mckenzie, J.A., Vasconcelos, C.: Microbial biomineralization processes forming modern Ca:Mg carbonate stromatolites. Sedimentology 57, 27–40. https://doi.org/10.1111/j.1365-3091.2009.01083.x, 2010.

Stockmann, G., Tollefsen, E., Skelton, A., Brüchert, V., Balic-Zunic, T., Langhof, J., Skogby, H., Karlsson, A.: Control of a calcite inhibitor (phosphate) and temperature on ikaite precipitation in Ikka Fjord, southwest Greenland. Appl. Geochemistry 89, 11–22. https://doi.org/10.1016/j.apgeochem.2017.11.005, 2018.

Suchý, V., Borecká, L., Pachnerová Brabcová, K., Havelcová, M., Svetlik, I., Machovič, V., Lapčák, L., Ovšonková, Z.A.: Microbial signatures from speleothems: A petrographic and scanning electron microscopy study of coralloids from the Koněprusy Caves (the Bohemian Karst, Czech Republic). Sedimentology 68, 1198–1226. https://doi.org/10.1111/sed.12826, 2021.

Teixeira, C.A.S., Sawakuchi, A.O., Bello, R.M.S., Nomura, S.F., Bertassoli, D.J., Chamani, M.A.C.: Fluid inclusions in calcite filled opening fractures of the Serra Alta Formation reveal paleotemperatures and composition of diagenetic fluids percolating Permian shales of the Paraná Basin. J. South Am. Earth Sci. 84, 242–254. https://doi.org/10.1016/j.jsames.2018.04.004, 2018.

Tisato, N., Torriani, S.F.F., Monteux, S., Sauro, F., De Waele, J., Tavagna, M.L., D'Angeli, I.M., Chailloux, D., Renda, M., Eglinton, T.I., Bontognali, T.R.R.: Microbial mediation of complex subterranean mineral structures. Sci. Rep. 5, 15525. https://doi.org/10.1038/srep15525, 2015.

Trampe, E.C.L., Larsen, J.E.N., Glaring, M.A., Stougaard, P., Kühl, M.: In situ Dynamics of O2, pH, Light, and Photosynthesis in Ikaite Tufa Columns (Ikka Fjord, Greenland)—A Unique Microbial Habitat. Front. Microbiol. 7, 128–143. https://doi.org/10.3389/fmicb.2016.00722, 2016.

Trichet, J., Défarge, C., Tribble, J., Tribble, G., Sansone, F., 2001. Christmas Island lagoonal lakes, models for the deposition of carbonate–evaporite–organic laminated sediments. Sediment. Geol. 140, 177–189. https://doi.org/10.1016/S0037-0738(00)00177-9

Turner, E.C., Jones, B.: Microscopic calcite dendrites in cold-water tufa: Implications for nucleation of micrite and cement. Sedimentology 52, 1043–1066. https://doi.org/10.1111/j.1365-3091.2005.00741.x, 2005.

Uriz, M.-J., Turon, X., Becerro, M.A., Agell, G.: Siliceous spicules and skeleton frameworks in sponges: Origin, diversity, ultrastructural patterns, and biological functions. Microsc. Res. Tech. 62, 279–299. https://doi.org/10.1002/jemt.10395, 2003.

Valdez Buso, V., Aquino, C.D., Paim, P.S.G., de Souza, P.A., Mori, A.L., Fallgatter, C., Milana, J.P., Kneller, B.: Late Palaeozoic glacial cycles and subcycles in western Gondwana: Correlation of surface and subsurface data of the Paraná Basin, Brazil. Palaeogeogr. Palaeoclimatol. Palaeoecol. 531, 108435. https://doi.org/10.1016/j.palaeo.2017.09.004, 2019.

Valdez Buso, V., Milana, J.P., di Pasquo, M., Paim, P.S.G., Philipp, R.P., Aquino, C.D., Cagliari, J., Junior, F.C., Kneller, B.: Timing of the Late Palaeozoic glaciation in western Gondwana: New ages and correlations from Paganzo and Paraná basins. Palaeogeogr. Palaeoclimatol. Palaeoecol. 544, 109624. https://doi.org/10.1016/j.palaeo.2020.109624, 2020.

Vasconcelos, C., McKenzie, J.A., Bernasconi, S., Grujic, D., Tiens, A.J.: Microbial mediation as a possible mechanism for natural dolomite formation at low temperatures. Nature 377, 220–222. https://doi.org/10.1038/377220a0, 1995.

Vasconcelos, C., Warthmann, R., McKenzie, J.A., Visscher, P.T., Bittermann, A.G., van Lith, Y.: Lithifying microbial mats in Lagoa Vermelha, Brazil: Modern Precambrian relics? Sediment. Geol. 185, 175–183. https://doi.org/10.1016/j.sedgeo.2005.12.022, 2006.

Verrecchia, E.P., Verrecchia, K.E.: Needle-fiber Calcite: A Critical Review and a Proposed Classification. SEPM J. Sediment. Res. Vol. 64A, 650–664. https://doi.org/10.1306/D4267E33-2B26-11D7-8648000102C1865D, 1994.

Vesely, F.F., Assine, M.L.: Deglaciation sequences in the Permo-Carboniferous Itararé Group, Paraná Basin, southern Brazil. J. South Am. Earth Sci. 22, 156–168. https://doi.org/10.1016/j.jsames.2006.09.006, 2006.

Vesely, F.F., Delgado, D., Spisila, A.L., Brumatti, M.: Divisão litoestratigráfica do das Grupo Itararé no Mapeamento da suscetibilidade vertentes naturais estado do Paraná translacionais em ante a ocorrência de escorregamentos um trecho da BR-376 , através da análise. Bol. Parana. Geosci. 78, 3–23, 2021.

Vickers, M., Watkinson, M., Price, G.D., Jerrett, R.: An improved model for the ikaite-glendonite transformation: evidence from the Lower Cretaceous of Spitsbergen, Svalbard. Nor. J. Geol. 98, 1–15. https://doi.org/10.17850/njg98-1-01, 2018.

Vuillemin, A., Wirth, R., Kemnitz, H., Schleicher, A.M., Friese, A., Bauer, K.W., Simister, R., Nomosatryo, S., Ordoñez, L., Ariztegui, D., Henny, C., Crowe, S.A., Benning, L.G., Kallmeyer, J., Russell, J.M., Bijaksana, S., Vogel, H., The Towuti Drilling Project Science Team.: Formation of diagenetic siderite in modern ferruginous sediments. Geology 47, 540–544. https://doi.org/10.1130/G46100.1, 2019.

W. C. Ward, R.B.H.: Dolomitization in a Mixing Zone of Near-Seawater Composition, Late Pleistocene, Northeastern Yucatan Peninsula. SEPM J. Sediment. Res. Vol. 55, 407–420. https://doi.org/10.1306/212F86E8-2B24-11D7-8648000102C1865D, 1985.

Wacey, D.: Stromatolites in the ~3400 Ma Strelley Pool Formation, Western Australia: Examining Biogenicity from the Macro- to the Nano-Scale. Astrobiology 10, 381–395. https://doi.org/10.1089/ast.2009.0423, 2010.

Wacey, D.: Establishing the Criteria for Early Life on Earth. pp. 47–53. https://doi.org/10.1007/978-1-4020-9389-0_4, 2009.

Warren, J.: Dolomite: occurrence, evolution and economically important associations. Earth-Science Rev. 52, 1–81. https://doi.org/10.1016/S0012-8252(00)00022-2, 2000.

Warren, J.K.: Evaporites through time: Tectonic, climatic and eustatic controls in marine and nonmarine deposits. Earth-Science Rev. 98, 217–268. https://doi.org/10.1016/j.earscirev.2009.11.004, 2010.

Warren, J.K.: Evaporites. Springer International Publishing, Cham. https://doi.org/10.1007/978-3-319-13512-0, 2016.

Weaver, C. E.: Shale-slate metamorphism in southern Appalachians. Elsevier, 1984.

Weaver, J.C., Morse, D.E.: Molecular biology of demosponge axial filaments and their roles in biosilicification. Microsc. Res.
1210 Tech. 62, 356–367. https://doi.org/10.1002/jemt.10401, 2003.

Weiner, S.: Biomineralization: A structural perspective. J. Struct. Biol. 163, 229–234.
https://doi.org/10.1016/j.jsb.2008.02.001, 2008.

Weiner, S., Dove, P.: An Overview of Biomineralization Processes and the Problem of the Vital Effect. Rev. Mineral.
Geochemistry 54, 1–29. https://doi.org/10.2113/0540001, 2003.

1215 Weinschütz, L. C., de Castro, J. C.: Seqüências deposicionais da Formação Taciba (Grupo Itararé, Neocarbonífero a
Eopermiano) na região de Mafra (SC), Bacia do Paraná. Brazilian Journal of Geology, 36(2), 243-252, 2006.

Westall, F.: Morphological Biosignatures in Early Terrestrial and Extraterrestrial Materials. Space Sci. Rev. 135, 95–114.
https://doi.org/10.1007/s11214-008-9354-z, 2008.

Westall, F., Folk, R.L.: Exogenous carbonaceous microstructures in Early Archaean cherts and BIFs from the Isua Greenstone
1220 Belt: implications for the search for life in ancient rocks. Precambrian Res. 126, 313–330. https://doi.org/10.1016/S0301-
9268(03)00102-5, 2003.

Whitney, D.L.: Coexisting andalusite, kyanite, and sillimanite: Sequential formation of three Al 2 SiO 5 polymorphs during
progressive metamorphism near the triple point, Sivrihisar, Turkey. Am. Mineral. 87, 405–416. https://doi.org/10.2138/am-
2002-0404, 2002.

1225 Wolf, K.H.: Gradational sedimentary products of calcareous algae. Sedimentology 5, 1–37. https://doi.org/10.1111/j.1365-
3091.1965.tb01556.x, 1965.

Worden, R.H., Burley, S.D.: Sandstone Diagenesis: The Evolution of Sand to Stone, in: Sandstone Diagenesis. Blackwell
Publishing Ltd., Oxford, UK, pp. 1–44. https://doi.org/10.1002/9781444304459.ch, 2009.

Wright, D.T., Wacey, D.: Sedimentary dolomite: a reality check. Geol. Soc. London, Spec. Publ. 235, 65–74.
1230 https://doi.org/10.1144/GSL.SP.2004.235.01.03, 2004.

Wright, D.T., Wacey, D.: Precipitation of dolomite using sulphate-reducing bacteria from the Coorong Region, South
Australia: significance and implications. Sedimentology 52, 987–1008. https://doi.org/10.1111/j.1365-3091.2005.00732.x,
2005.

Wright, V.P., Barnett, A.J.: An abiotic model for the development of textures in some South Atlantic early Cretaceous
1235 lacustrine carbonates. Geol. Soc. Spec. Publ. 418, 209–219. https://doi.org/10.1144/SP418.3, 2015.

Xia, C., Ye, B., Jiang, J., Hou, Z.: Review of natural origin, distribution, and long-term conservation of CO2 in sedimentary
basins of China. Earth-Science Rev. 226, 103953. https://doi.org/10.1016/j.earscirev.2022.103953, 2022.

Xu, F., You, X., Li, Q., Liu, Y.: Can primary ferroan dolomite and ankerite be precipitated? Its implications for formation of
submarine methane-derived authigenic carbonate (MDAC) chimney. Minerals 9. https://doi.org/10.3390/min9070413, 2019.

1240   Zalán, P. V., Conceição, J. J., Astolfi, M. M., Tiriba Appi, V., Wolff, S., Santos Vieira, I.: Estilos estruturais relacionados a intrusões magmáticas básicas em rochas sedimentares. Boletim Técnico da Petrobrás, (4), 221-230, 1985.

Zekri, A.Y., Shedid, S.A., Almehaideb, R.A.: Investigation of supercritical carbon dioxide, aspheltenic crude oil, and formation brine interactions in carbonate formations. J. Pet. Sci. Eng. 69, 63–70. https://doi.org/10.1016/j.petrol.2009.05.009, 2009.

Zhang, Y., Sun, H., Stowell, H.H., Zayernouri, M., Hansen, S.E.: A review of applications of fractional calculus in Earth

1245   system dynamics. Chaos, Solitons & Fractals 102, 29–46. https://doi.org/10.1016/j.chaos.2017.03.051, 2017.

Zhou, X., Lu, Z., Rickaby, R.E.M., Domack, E.W., Wellner, J.S., Kennedy, H.A.: Ikaite Abundance Controlled by Porewater Phosphorus Level: Potential Links to Dust and Productivity. J. Geol. 123, 269–281. https://doi.org/10.1086/681918, 2015.

Zhu, L., Zhao, Q., Zheng, X., Xie, Y.: Formation of star-shaped calcite crystals with Mg2+ inorganic mineralizer without organic template. J. Solid State Chem. 179, 1247–1252. https://doi.org/10.1016/j.jssc.2006.01.036, 2006.